This is a repository copy of *Review of gas emissions from lithium-ion battery thermal runaway failure — considering toxic and flammable compounds*.

Article:

Review article

Review of gas emissions from lithium-ion battery thermal runaway failure — Considering toxic and flammable compounds

Peter J. Bugryniec [a], Erik G. Resendiz [a], Solomon M. Nwophoke [a], Simran Khanna [b], Charles James [c], Solomon F. Brown [a,*]

[a] *Department of Chemical & Biological Engineering, University of Sheffield, Sheffield, S1 3JD, UK*
[b] *Department of Materials, Imperial College London, London, SW7 2AZ, UK*
[c] *School of Chemistry, University of St Andrews, St Andrews, KY16 9ST, UK*

ARTICLE INFO

ABSTRACT

Lithium-ion batteries (LIBs) present fire, explosion and toxicity hazards through the release of flammable and noxious gases during rare thermal runaway (TR) events. This off-gas is the subject of active research within academia, however, there has been no comprehensive review on the topic. Hence, this work analyses the available literature data to determine how battery parameters affect the variation in off-gas volume and composition, to determine the flammability and toxicity hazards of different battery chemistries. It is found on average that: (1) NMC LIBs generate larger specific off-gas volumes than other chemistries; (2) prismatic cells tend to generate larger specific off-gas volumes than offer cell forms; (3) generally a higher SOC leads to greater specific gas volume generation; (4) LFP batteries show greater toxicity than NMC; (5) LFP is more toxic at lower SOC, while NMC is more toxic at higher SOC (respective to themselves); and (6) LFP off-gas has a greater flammability hazard. Further, recommendations are presented so that significant improvements in research can be made to advance the understanding of LIB off-gas further. Finally, this work is a critical resource to the battery community to aid the risk assessment of LIB TR fire, explosion and toxicity hazards.

1. Introduction

As with traditional transportation fuels (i.e. hydrocarbons such as petrol and diesel), electrochemical energy sources like Li-ion batteries (LIBs) have inherent safety risks related to fire and toxicity [1–5]. The maturity of the internal combustion engine (ICE) means that the hazards of vehicle fires under different scenarios are well understood. However, with the accelerating uptake of LIB-powered electric vehicles (in the road, rail and marine sectors) there is a concern that there will be a growing knowledge gap between understanding the hazards of traditional and alternative fuel vehicles [6]. There have been several reviews of the growing literature on LIB safety, focusing on the mechanisms of cell thermal runaway (TR) and fire phenomenon [6,7]. However there are no reviews that specifically and comprehensively analyse LIB off-gas which is known to be flammable (containing hydrogen and hydrocarbons) leading to explosion and loss of life [8,9]. Further, for those involved in or near a TR event, toxic gas emissions (e.g. CO and HF) present an additional threat. However, the composition of the off-gas is complex and needs extensive consideration.

The risk of fire, explosion or vapour cloud ignition extends to stationary energy storage, EVs and marine applications, where incidents have occurred in reality [e.g. 9–11], showing that this is a real and present hazard. Adequate risk assessments are required to manage and mitigate this fire/explosion hazard and to aid emergency responders in understanding hazards they may walk into [12,13]. However, this can only be done with accurate and extensive knowledge of the off-gas volume and components (i.e. H_2, hydrocarbons, flammable solvent vapours, CO_2 dilution effect) to determine the explosion potential of the off-gas in a given scenario. This is also true for the toxicity of the off-gas, where determining the extent to which individuals are at risk of breaching *Immediate Danger to Life and Health* or exposure limits is essential. For example, in scenarios where individuals are exposed to off-gas in confined spaces, such as from the failure of personal transport stored in the home [14,15] or EV failure in a car garage [4,16]. As will be shown below, there is no extensive analysis of LIB off-gas considering the influence of battery variables, which is necessary for a thorough understanding of its hazards.

There has been some work to understand the overall off-gas behaviour. Baird et al. [17] compiled the gas emissions of ten papers

---

Nomenclature

DEC	Diethyl carbonate
DMC	Dimethyl carbonate
EC	Ethylene carbonate
EMC	Ethyl methyl carbonate
EV	Electric vehicle (automotive)
HRR	Heat release rate
ICE	Internal combustion engine
IQR	Inter quartile range
LCO	Lithium cobalt oxide
LFL	Lower flammability limit
LFP	Lithium iron phosphate
LIB	Lithium ion (Li-ion) battery
LMO	Lithium manganese oxide
LTO	Lithium titanate
NCA	Lithium nickel cobalt aluminium oxide
NMC	Lithium nickel manganese cobalt oxide
PC	Propylene carbonate
SEI	Solid electrolyte interphase
SOC	State of charge
THC	Total hydrocarbons
TR	Thermal runaway

showing gas composition related to different cell chemistries and SOC, while Li et al. [18] compiled the gas emissions of 29 tests under an inert atmosphere. However, in both cases, no analysis is made relating chemistry, SOC, etc. to off-gas composition. Instead, flammability limit calculations and flame speed analysis were conducted. The most compressive review to date is by Rappsilber et al. [19] who analysed 76 papers focusing on peak heat rate, total heat, CO emission, total gas volume, and HF production. However, the overall volume and specific CO emissions trends are determined by grouping all the cell chemistry data for each SOC, while for HF only LFP cells are analysed.

This work aims to address the lack of a comprehensive review of LIB gas emissions during TR via collating and analysing data available in the literature. Within this aim the objectives are to understand how battery parameters affect the variation in off-gas volume and composition, and what battery can be considered least hazardous. Overall it provides a crucial resource that can be used in the risk assessment of LIB TR fire and explosion hazards.

The remainder of the introduction will outline the demand for LIBs, explain what a LIB is and describe the hazardous thermal runaway phenomenon. Section 2 will then review the literature on LIB off-gas composition and toxicity. In Section 3 the methods are presented for gathering and processing the literature data. Section 4 presents the analysis and discussion of the literature data. Section 5 provides concluding remarks.

1.1. Overview of lithium-ion batteries and thermal runaway

From powering personal electronics devices, LIBs are becoming the widely adopted energy source for automotive electric vehicles (EVs) and personal transport (bicycles and scooters). They are also increasingly used in ships and trains as auxiliary or primary power sources. Further, the aviation sector is also developing EVs based on LIB energy sources for electric vertical take-off and landing (eVTOL) as well as for light/short hall aircraft. Lastly, LIBs are also used in commercial battery energy storage (BESS) for grid support as well as domestic energy storage. With such growing use in terms of quantity and scale, there are increasing opportunities for LIB failure to cause greater harm. This is specifically true in certain situations where failure is more critical,

such as in the marine and aviation sector where there is limited scope to distance people and assets from the failure.

LIBs are widely used as they have a high energy density, long cycle life and are low cost. Cell performance can be altered by materials selection, with common cell chemistries consisting of lithium cobalt oxide (LCO), lithium iron phosphate (LFP), lithium manganese oxide (LMO), lithium nickel cobalt aluminium oxide (NCA), lithium nickel manganese oxide (NMC) and lithium titanate (LTO). Generally NMC and NCA are used as high-energy cells, while LFP cells have a lower specific energy capacity but a larger specific power capacity and longer life span [20]. Further, battery performance (energy and power capabilities) is scalable by the number and configuration (series and parallel connections) of cells. Cells can be manufactured in different forms, commonly cylindrical, pouch or prismatic with capacities ranging from 1 Ah to 300 Ah. These characteristics allow LIBs to be customised for the variety of different applications mentioned above. However, even with these advantages, LIBs suffer from the phenomenon of thermal runaway (TR), explained in the next section.

1.1.1. LIB thermal runaway

The process of TR, see Fig. 1, involves the exothermic chemical decomposition of the battery cell materials leading to vast heat generation and temperature rise. This is accompanied by the generation of gasses from the decomposition process that can be flammable and toxic, and can lead to smoke, hot sparks and jet flames ejected from the cell [6]. Many reactions take place during the decomposition of the cell; however, the main stages consist of solid electrolyte interphase (SEI) breakdown, anode-electrolyte reaction, cathode-electrolyte reactions and electrolyte decomposition, see Table 1 for further details. Further, in a module or pack the heat from one cell can cause a cascading failure or propagation throughout the pack, increasing the overall hazard from failure. For module or pack failure this includes the production of large amounts of flammable gas that can lead to explosions [8,9].

Typically this occurs when the off-gas is confined to an enclosed space, thus not naturally dissipating like in the open, and either (1) an ignition source occurs when the fuel-air ratio is in the explosion range [8]; or (2) if additional air is allowed to enter (by opening a door to address the failure [9]) bringing the fuel-air ratio from above the upper explosion limit (UEL) into the explosion range. However, at least one unconfined off-gas explosion has taken place, where a large cloud of smoke accumulating around an electric bus suddenly erupts in flames [10], indicating that this smoke is a vapour cloud igniting [21]. This behaviour is complex, so to understand this hazard more it is important to determine how much volume and what species of gases are generated for different cell chemistries, forms, SOC, scale (cell/module/pack) and abuse.

2. Gas generation and toxicity — literature review

This section summarises the findings of individual literature sources regarding volume of gas produced (Section 2.1), gas composition (Section 2.2), toxicity (Section 2.3), presence of electrolyte vapour (Section 2.4), other influential factors including the effect of abuse scenarios (Section 2.5) and results from module and pack tests (Section 2.6).

2.1. Gas volume produced

The volume of gas LIBs generate during TR can be influenced by several conditions, including capacity, SOC and chemistry. At 100% SOC LFP cells are shown to generate a lower volume of gas than other chemistries (LCO, NMC, LMO), 0.4 L/Ah to 1.4 L/Ah versus 1.28 L/Ah to 21 L/Ah respectively [24–32]. In contrast, large NMC prismatic cells (41 Ah) and LFP cells (5.5 Ah) have been shown to generate similar off-gas volumes, 1.64 L/Ah and 1.83 L/Ah respectively (in nitrogen) [33]. While, LTO cells have been shown to generate significantly more off-gas than LFP cells, but less than NMC [34]. Further, higher nickel-content
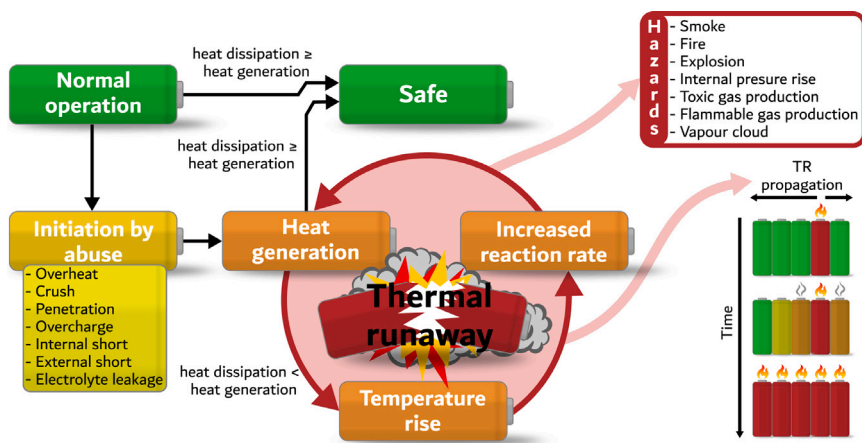
Fig. 1. Process of thermal runaway from initiation to propagation and resulting hazards [22].

Table 1
Summary of main reactions of LIB cell TR failure.
Source: Edited from [23].

Temperature (°C)	Reaction behaviour
>70	Li salt decomposition and reaction with solvent and Solid electrolyte interphase (SEI)
90–130	SEI breaks down leading to anode-electrolyte reaction. Low heat generation.
90–230	Li-electrolyte reaction occurs, leading to gas production e.g. C_2H_4, C_2H_6 and C_3H_6.
120–220	Electrolyte vaporises, leading to additional gas generation, cell pressurisation and initial venting. Separator melts at 130°C to 190°C.
160	Heat generation increases — from "self heating" to "thermal runaway". Violent gas and particle release (second venting).
200–300	Electrolyte decomposition occurs. At TR there is a rapid temperature rise, the metal oxide cathode decomposes to produce oxygen. O_2 leads to the oxidation of the electrolyte -> CO_2 and H_2O

NMC cells produce more gas than counterparts with less nickel [31,32]. Overall, the absolute vent gas volume increases with capacity [31, 32,35]. Limited work has compared cell forms, but NMC pouch and prismatic cells have been shown to generate similar volumes of gas production [36].

In many studies gas volume production is shown to increase as SOC increases for various chemistries, including NMC [23,30,37–39], LFP [25,40], NCA [25] and LCO [26]. However, little to no correlation between gas volume and SOC is observed in some studies on LFP and NMC cells [25,41]. Further, the greatest increase in emissions is typically seen over the range of 50% to 100% SOC [7,30]. Also, the increase in gas production with SOC has shown to be greater for NCA than for LFP cells. While at higher SOC LFP is typically shown to produce less off-gas than other chemistries, at lower SOC volumes can be comparable between chemistries, but in some cases LFP can generate more [7,25]. Increased gas generation at higher SOC is attributed to higher electrode potentials and more reactive cell materials [7]. The occurrence of combustion may also have an effect. When the failure of NMC cells did not lead to combustion (at 0% SOC) more gas production was recorded [41].

The peak rate of gas production has been shown to be proportional to SOC [7,39], while in other work this is not true [42]. Peak gas rates of individual species (CO, CO_2 and HF) have been shown to increase with SOC [43].

2.2. Gas composition

The main components of the off-gas are CO_2, CO, H_2 and hydrocarbons, while under certain conditions significant amounts of electrolytes and water can be present. The list of hydrocarbons generated can be many, but those typically measured/reported are CH_4, C_2H_6, C_2H_4, C_2H_2, C_3H_6 and C_3H_8. Further, there are possibly hundreds of components present in the off-gas, including non-hydrocarbons and toxins, that are infrequently reported [44–46]. The toxic components of main concern are CO, HF, HCl, HCN, NO_x, and SO_2 [7]. Table 2 summarises the hazards and exposure limits of the main off-gas components. Exposure limits are the concentrations of hazardous substances in air, averaged over 8 h or 15 min (long-term and short-term limits respectively), that are set to prevent harmful effects on people's health [47]. The reaction mechanisms towards species production are well discussed in the literature [see, for example, 24,25,32,37,48–51] and are not a topic for discussion here.

Comparing the off-gas composition from different sources highlights the variation in components and their volume fractions between and within chemistries. Typically, literature sources identify LFP as generating more CO_2 and H_2 than other chemistries that generate mostly CO and THC, in terms of volume fraction [24,32,34,56]. However, high levels of H_2, CO_2 and lower levels of CO have been reported in NMC cells [33], while higher CO_2 volumes have been reported for NCA compared to LFP cells [25]. It has been reported that the percentage of CO and H_2 production is proportional and inversely proportional to energy density, respectively [32]. This inherently links to nickel content for the NMC cells; however, later work shows less correlation [31]. Further, comparing solid-state cells versus "typical" Li-ion cells shows a reduction in gas production (by 10%) and a lower proportion of THC and H_2 (by 30% each), while the proportions of CO_2 and CO are larger (by 20% for CO) for the solid-state cells [57].

Koch et al. [27] have done one of the most extensive testing regimes of 51 NMC cells ranging from 20 Ah to 80 Ah. Significant amounts of

Table 2

Common LIB off-gas components, hazards and exposure limits.

Substance	Hazard[a]	Exposure Limit, 8 h (mg/m^3)[b]	Exposure Limit, 15 min (mg/m^3)[b]
Carbon dioxide, CO_2	Cause headaches, dizziness, confusion, loss of consciousness, and asphyxiation at high concentrations [52].	9150	27 400
Carbon monoxide, CO	Toxic if inhaled, may damage the unborn child, causes damage to organs through prolonged or repeated exposure and is an extremely flammable gas.	23	117
Hydrogen, H_2	Extremely flammable.	See note[d]	
Hydrocarbons	Flammable.	See note[d]	
Hydrogen fluoride, HF	Fatal if swallowed, is fatal in contact with skin, is fatal if inhaled and causes severe skin burns and eye damage.	1.5	2.5
Hydrogen chloride, HCl	Severe skin burns and eye damage, is toxic if inhaled, may damage fertility or the unborn child, causes serious eye damage, may cause damage to organs through prolonged or repeated exposure, may be corrosive to metals, may cause respiratory irritation and contains gas under pressure and may explode if heated.	2	8
Hydrogen cyanide, HCN	Fatal if swallowed, is fatal in contact with skin, is fatal if inhaled, causes damage to organs through prolonged or repeated exposure, is very toxic to aquatic life (with long lasting effects) and is an extremely flammable liquid and vapour.	1	5
Nitrogen dioxide, NO_2	Fatal if inhaled, causes severe skin burns and eye damage; and may cause or intensify fire (oxidiser).	0.96	1.91
Sulphur dioxide, SO_2	Severe skin burns and eye damage and is toxic if inhaled.	1.3	2.7
Solvents	Highly flammable liquid and vapour [53]. Very irritating to eyes, skin and airways [44].	DEC 700, PC 8.5[c]	DEC 1000, PC 8.5[c]

[a] Cited from the European Chemicals Agency [53], unless otherwise stated.

[b] Cited from the HSE [47], unless otherwise stated.

[c] Cited from the IFA [54] for the solvents DEC (Romania) and PC (Germany), other common electrolyte solvents (e.g. EC and DMC) are not listed.

[d] Hydrocarbons, such as CH_4, are described as acting as simple asphyxiants without other significant physiologic effects when they are present in high concentrations, hence are not given limit values as the significant factor is the availability of oxygen [55]. This is assumed for H_2 as well.

CO_2 are recorded at low-vent gas volumes as combustion could still be complete even in the limited oxygen availability of the closed system. Koch et al. found that (for vent gas volumes greater than 50 l where combustion was limited) 7 components make up over 99% of the off-gas volume. These components (and their average volume proportions) are CO_2 (36.6%), CO (28.3%), H_2 (22.3%), C_2H_4 (5.6%), CH_4 (5.2%), C_2H_6 (1.0%) and C_3H_6 (0.5%). These averages have a large variation, with CO, CO_2 and H_2 being within the error of each other. Further, there is no correlation between composition and the vent gas volume.

SOC is shown to affect the off-gas composition ratio and the number of components produced. At 0% SOC the gas can be mainly CO_2 [17], or a few components (~5) including CO and solvents, while this can reach several tens of components at higher SOC [58]. Generally, it has been found that the percentage volume of CO_2 in the off-gas reduces while CO increases as SOC increases for various chemistries (LCO, NCA, LFP) [7,17,25,26,59]. At the same time, THC and H_2 have been found to remain steady across SOC for LCO cells [26]. For LFP and NCA cells H_2 is seen to increase in volume fraction [25], while H_2 and THC are found to increase in volume fraction for LCO and LFP cells [17], with SOC. However, other works have shown contradictory results, where CO_2 increases and THC reduces with SOC increase [37], or the fraction of THC reduces along with CO_2 with SOC increase [59]. Also, H_2 was only detected at 100% for LFP cells [42].

Peak concentrations of gases and production rates increase with SOC [39,60,61]. However, the reduction of CO_2 volume fraction can be attributed to the increase in absolute production of other gases while CO_2 concentration remains stable [60,62]. The reduction of hydrocarbons and increase in CO and CO_2 at higher SOC (in a nitrogen atmosphere) has been attributed to combustion events [37,39], however Willstrand et al. [7] shows contradictory behaviour. Nevertheless,

it has been noted that higher SOC enhances combustion, leading to a greater HRR and higher concentrations of CO_2 and CO [63,64]. More so, the relationship of combustion efficiency (turning CO to CO_2) is complex and dependent on temperature (generally proportional to SOC), abuse method, oxygen availability and gas generation rate [7].

Studying the flammability limit of cell off-gas, for NMC cells (18650, 3.5 Ah) the lower explosion limit (LEL) increases up to a maximum of 10.15% at a SOC of 50% and then reduces at higher SOC, while the upper explosion limit (UEL) continually increases [65]. This means a SOC of 50% has the lowest risk of combustion in an open space. However, the narrowest flammability range is at a SOC of 30%, hence this SOC is recommended for the storage and transport of LIBs. The trend in LEL is attributed to the change in multi-carbon chain gas components. When there are more gas components with longer carbon-chains the LEL reduces.

Electrolyte composition is shown to affect the off-gas from cell abuse. For different LFP 18650 cells, where EMC is always present and makes up approximately 50% of the electrolyte solvent, there is a weak trend between increased EMC proportion and reduced gas generation, while the percentage of CO_2 increases with increased EMC proportion [66]. Studies on electrolytes alone have shown that the concentration of lithium salt affects the ratio of off-gas species, while an increase in salt concentration leads to greater instability and gas production [67]. The individual solvents (e.g. EC, DEC, EMC and DMC) also vary in stability and gas volume production, with EC and DEC being the least thermally stable and reactivity increasing with the addition of $LiPF_6$ salts [68]. Further, the use of binary mixtures leads to electrolytes that have stability broadly related to the solvent-mole ratios. For EC, EMC and DMC solvents with 1.2M $LiPF_6$ gas emissions are dominated by CO_2 (70%), but for DEC (1.2M $LiPF_6$) CO_2 and C_2H_6

account for 30% each; however, tens of components are recorded in total in all cases. Similar behaviour has been shown by Fernandes et al. [69], but with thermal decomposition of EMC and particularly DMC occurring at lower temperatures. Further, there is uncertainty in the actual reaction mechanism for the thermal decomposition of battery solvents [70].

Additionally, the presence of the cathode and anode materials in a cell complicates the reaction behaviour. Intercalated lithium in the anode can react with the solvents to produce hydrocarbons, while oxygen released from the cathode decomposition can lead to decomposition [71,72]. The reaction pathways to gas generation are numerous and complex and the readers are referred to existing reviews on the mechanism of thermal runaway, see Refs. [71,72]. Additives have also been used to improve anode-electrolyte stability and impede fires [73]. Flame retardants can reduce fires leading to less CO_2 but more H_2 and CO. Further, in the near future it is expected that all-solid-state cells will be commercial, in which their solid electrolyte has increased stability and reduced heat of reaction, dramatically improving cell safety but with little know of the amount and type of gas produced [74]. Due to these numerous variables (i.e. solvents, solvent ratios, salt concentrations and additives) and that few works know or record the electrolyte composition in battery safety/off-gas tests, electrolyte composition is not considered in further discussions as a variable affecting off-gas characteristics.

2.3. Toxicity

Several toxic compounds commonly discussed include CO, HCl, HCN, NO, SO_2, HF, fluorinated carbonates, POF_3, COF_2, acrolein, and formaldehyde [29,38,50,60,61,75–77]. Non-quantified work has detected up to 35 toxic substances which vary with chemistry and SOC [78]. Understanding the presence of these compounds is important as inhalation of these gasses can result in dizziness, headache, loss of consciousness, coma or even death [6].

The risks of these emissions, however, depend on the scenario of the incident. In the outside environment, HF will likely rise and quickly dissipate. Whereas, in enclosed spaces HF will increase and be problematic if gasses are not evacuated. More full-scale tests are needed to fully establish this and assess the effects of fire suppression on toxicity.

For LMO cells the total amount of HCl generated remains stable with SOC but the amount of SO_2 increases with SOC, while NO shows no correlation [60]. The change in HCN concentration is also shown to be minimal over increased SOC [38]. For NMC prismatic cells (94 Ah), more SO_2 was produced at 50% SOC than at 100% SOC while the maximum temperature was 510°C compared to 620°C, respectively [77]. The rate of HF production increases with SOC [61,75,76], while for a stack of LFP pouch cells the peak HF production rate is seen at 50% SOC [79].

For LCO, NCA and LFP cells, it is shown that there is a downward trend of specific HF production with SOC increase [50,60,61,75]. In some cases for LFP cells, HF is only detected at low SOC (at or below 25% SOC) [7]. However, peak HF production for LFP cells has been seen at 50% SOC [79] or 100% SOC [80]. Also, CO and HF production has been shown to increase with SOC (for 22 Ah LFP cells) [42].

Comparing HF production between cell chemistries, LCO prismatic and LFP cylindrical cells are shown to produce similar specific amounts of HF, so do NCA and LFP pouch cells [76], as well as LFP and LMO/NMC [29]. However, Sturk et al. [75] show that LFP cells generate significantly more HF than their NMC counterparts. HF is found to be the largest contributor to toxicity for LFP cells, while for LCO and NMC it is Acrolein [50]. From this, LFP cells produce the largest theoretical contamination volume (300 m^3) versus LCO and NMC cells (200 m^3) (considering 18650 cells). Overall, there is no strong trend for the theoretical contamination value with SOC, because as HF decreases with SOC there is an increase in other toxins such as CF_4.

For other toxins, the number of combustion organic products increases with SOC, up to a SOC of 100%, and then there is a significant reduction at a SOC of 150% [81]. In total, over a hundred species were detected, but more products are seen in LCO, NMC and LMO cells than in LFP cells. For NMC and LCO cells a higher SOC showed more substances, while for LFP cells the greatest amount of substances was detected at 30% SOC [78]. Six very toxic substances identified as 2-propenal, methyl vinyl ketone, propanedinitrile, propanenitrile, 1,2-dimethyl-hydrazine and thiocyanic acid ethyl ester could be detected. Further, phosphonofluridates have been detected in NMC but not LFP cells [44].

The cell form may influence HF production. LFP pouch cells are shown to produce an order of magnitude more HF than cylindrical cells [60,76]. However, NMC pouch and prismatic cells show similar volumes and composition of gas, including HF [36]. Further, abuse type can affect toxic gas generation. Thermal abuse produces a greater contamination volume than nail penetration, as penetration overall produces less gas [50].

While the dependence of SO_2 generation on SOC is not definitive, one theory attributes it to the fact that the formation of SO_2 requires significant heat [60]; hence, it only occurs at higher SOC where the TR temperature is higher. Conversely, less HF is theoretically formed at higher SOC as the higher TR temperatures promote bond breaking leading to the production of smaller molecules [50], or give rise to more complete burning [82] where the reaction between HF and hydrocarbons can consume the free HF [83], aided by the increase of hydrocarbons at higher SOC. The increase of CF_4 with SOC is not explained [50]. The fluorine within the cell materials can also lead to POF_3, from reaction with water, which may be more toxic than HF [6]. Even though HF has a high toxicity rating, the large amounts of CO make this the main toxicity concern [84].

2.4. Electrolyte vapour

During TR, the electrolyte can exist in the off-gas as a vapour and presents additional flammability, irritability and toxicity hazards. The combined off-gas/electrolyte mixture is sometimes termed the "vapour cloud" [21] and can exist due to a lack of heat initiating combustion or due to a lack of oxygen limiting oxidation such that the solvent remains as a fume [45].

The solvents DMC, EMC and DEC (common in electrolytes) are highly volatile with low boiling points of 90°C to 129°C and high relative evaporation rates (between 1 and 3) [85]. PC and EC can be considered less volatile with higher boiling points of 242°C to 249°C and lower relative evaporation rates (<0.005). The vapour densities of solvents used in Li-ion cells are heavier than air and so will accumulate at the ground when the liquid solvent evaporates. However, the relative vapour density (ρ_{rel}) for a chemical compared to air (where $\rho_{rel} = 1$, $\rho_{rel} < 1$ and $\rho_{rel} > 1$ would correspond to a vapour that is neutral, buoyant and dense respectively) depends on the molecular weight of the vapour, temperature of the vapour, temperature of the air and the saturated concentration of the vapour in the air [86]. Therefore, the behaviour of a TR event, i.e. the temperature of failure (influencing vapour temperature), the rate and magnitude of vapour discharge and the rate of vapour dispersion, will influence how the relative vapour density changes with time. Further, the presence of solvents still in the liquid state, as aerosols, can lead to a cloud initially behaving as dense due to the relatively heavy droplets even if the emitted vapour mixed with air would normally (initially) be buoyant or dense [86]. As such, initially buoyant clouds can turn dense and vice-versa, adding further complexity to understanding and predicting the hazard of vapour cloud explosions in relation to LIBs.

For the common electrolyte carbonates, the volume of solvent required to evaporate to reach hazardous levels with mild transient effects (within a 1-meter distance from a vehicle) is 2.24 mL, 1.40 mL, 0.17 mL, 0.13 mL for DMC, EC, PC and DEC respectively. Lithium salts

lead to HF production, which is toxic and corrosive: 20 mL of 1 M LiPF$_6$ electrolyte can release enough HF in a 62 m^2 room to cause serious permanent health effects. Further, Diaz et al. [50] have shown that a single 18650 cell can lead to a contaminated volume of 100 m^3 to 400 m^3 based on the off-gas considering emitted solvents, CO, HF and other toxic components.

Although the presence and hazards of the electrolyte vapour are known, it is not frequently measured in gas analysis studies. However, overcharging of LFP cells shows that the off-gas can have a composition that is 60% electrolyte (where no fire or burning is noted in this test) [48]. Other work has detected, but not quantified, the existence of the solvents [7,29,87]. For various cell chemistries, the most abundant compounds were stated to be carbonates, which for LFP cells were DEC and EMC, and for NMC cells where DMC and EMC [44].

2.5. Composition in relation to other factors

The composition of off-gas is shown to vary with different stages of TR. At initial venting, CO$_2$ dominates, followed by hydrocarbons and a minimal amount of H$_2$ [88,89]. In some cases, electrolyte solvents are recorded and in a significant quantity, while in others, H$_2$ is not present [23,37,48]. During TR there is a marginal increase in H$_2$, while during the deflagration there are significant amounts of CO and H$_2$ [88]. Also, electrolyte solvents are not recorded after TR [23]. However, aged cells show more CO and hydrocarbons at venting compared to fresh cells [89].

Other phenomena exist, including the retentively cool off-gas released early on in TR (compared to later stages) sinking to the floor (due to the vapour densities of solvents) [41]. Comparing "standard" versus "violent" TR, where violent is defined as maximum cell temperature over 250°C and more than 0.5 l of off-gas, there is more CO$_2$ and H$_2$ in violent cases [90]. LFP cells show no visible outburst of gas at SOC lower than 50% [82]. Similarly, for large LFP cells no fire or TR is seen at 0% SOC, but at 50% and above sustained jet fires are present [42].

The volume of gas produced by different abuse methods has been compared. Abuse by puncture (from projectile) shows less gas production than other failure modes (wedge-shaped penetration, impact and thermal) [2]. Different thermal abuse methods are shown to lead to similar results, except for reactor heating (where decomposition of electrolyte solvent occurs on the hot reactor walls after venting) leading to more gas being produced [28]. However, other work shows that a greater heating rate increases gas generation volume [90]. It is suggested that more gas is produced in air (allowing for combustion) than in a nitrogen atmosphere because the pyrolysis of organics produces a solid char [50]. Overcharge is shown to generate more gas (by more than 50%) than over-temperature or nail penetration [36]. Aged cells, with less remaining capacity, show less gas generation as more electrolyte is consumed in cells with less remaining capacity [91]. On overcharge, more gas is generated as a cell is increasingly overcharged [92], with the amount of CO$_2$ increasing at a greater rate than other gases (CO, H$_2$ and THC) [66,92,93]. However, Willstrand et al. [7] did not show any evidence to suggest that the abuse method affects the total gas volume produced or composition; but the abuse type does affect gas production rate, mass loss, and maximum temperature of the cell as much as its state of charge.

In open space, less gas is produced at a lower rate with the exception of CO$_2$ which has a higher rate [39]. Suggesting that more complete combustion occurs in open space, which conversely implies cells in a pack may not undergo complete combustion. In a nitrogen atmosphere hydrocarbons form a greater percentage of the off-gas than when abused in air [37]. For short circuit tests, more gas is produced in a nitrogen atmosphere and mainly consists of H$_2$, CO$_2$, CO and CH$_4$, while in air the off-gas is mostly CO$_2$ and CO [94]. However, repeats of the same test can result in significant differences in results [95].

2.6. Abuse at larger scales

Studying the TR of LIBs at different scales, i.e. from cell to module and pack level, is important to understand how the hazards scale with battery size. However, only a few academic studies focus on the pack (i.e. EV) level concentrating on fire and toxicity behaviour.

EV fire safety has focused on similar gases to research on a cell level, namely CO$_2$, CO, THC, NO$_x$, HF, HCl, HCN and heavy metals. The overall gas composition is similar between ICE and EVs. Over 95% of the combustion gas is CO$_2$, a few percent is CO and less than 0.5% is THC, HCl, HF, NO$_x$ and SO$_x$ individually [1,3,4]. The most significant difference in EV and ICE vehicle toxicity is the quantity of HF. Lecocoq et al. [3] and Truchot et al. [1] both show that EVs generate double the amount of HF than ICE vehicles (1.5 kg versus 0.7 kg), while Willstrand et al. [4] show that EVs generate an order of magnitude greater HF than ICE vehicles (0.7 kg versus 0.01 kg). Further, the peak HF generation rate (3 g/s to 4 g/s) is similar in both EV and ICE vehicles, attributed to the rupture of the air-conditioning refrigerant [1,3]. However, the HF generation rate is greater for EVs than ICE vehicles (1 g/s versus 0 g/s to 0.5 g/s) at times later on in the vehicles burning — presumably due to the battery burning. HCl percentage composition is similar between vehicle types. In addition to gas production, battery fires lead to heavy metal deposits [2] that results in more heavy metals being produced in greater quantities by EV fires [5]. Due to the low toxic thresholds of these toxic substances, it is important to consider them for toxic evaluation, even though the total amounts produced are low [1].

Further to this discussion, it should be stated that these EV studies consider abuse leading to TR leading to fire, and not any situation where there is TR without fire. However, it is noted that there have been instances in the public where EVs have gone into TR without fire until the ignition of the off-gas [96]. Hence, there is a need to understand why and how large-scale battery TR failure leads straight to fires in some instances and to gas emissions and explosion hazards in others.

Moving up the battery scale (from cell to stack to module) an increasing volume fraction of CO, CO$_2$, and H$_2$O is observed [8]. Further, the release of HF increases as module size increases, presumably due to simultaneous cell burning [75]. The production of gas (specific to capacity) is greater for a group of 10 cells with a similar capacity to one large cell, the gas production is 25% more at 100% SOC [97]. However, at 75% and 50% SOC there is a negligible difference between the group of cells and a single large cell. An array of the same capacity of a cell shows a tendency for higher CO$_2$ and CO fraction, with less H$_2$. Further, in general, the greater number of cells and cell capacity leads to greater EV fire risk [6]. However, it is shown heat release rate (HRR) does not scale linearly with capacity, because not all cells burn at once. Hence, one should take caution scaling other hazards relating to batteries linearly with capacity.

2.7. Summary

In general, cell capacity and energy density are influencing factors of TR behaviour, affecting emitted venting gas volume, self-heating onset temperature and cell mass loss [27]. On a cell level, gas production typically ranges from 1 l/Ah to 3 l/Ah given all chemistries and in absolute terms increases with cell capacity. Under direct comparisons, LFP cells produce less gas than other chemistries in most studies. However, separate studies show that LFP may produce gas (l/Ah) on a similar scale to high-energy cells. Further, many studies have shown that gas production increases with SOC, but this is not true in all studies nor for all chemistries.

The off-gas mainly consists of CO$_2$, CO, H$_2$ and hydrocarbons. However, the composition from the same as well as different cell chemistries and SOC varies considerably. The availability of oxygen (i.e. air vs inert atmosphere, or open vs closed space) affects the composition. Electrolytes can make up most of the off-gas but they are rarely

recorded. Given an abuse scenario, the composition is also different depending on how violent and hot the TR event occurs. Limited data on the overcharge of NMC cells shows more CO_2 is generated at higher SOC, while for LFP electrolyte vapours are the main component. The composition of the off-gas changes throughout TR, early on at low temperatures the initial venting can be mainly CO_2, solvents or CH_4 (dependent on chemistry). This implies the hazard assessment should consider the different stages in TR and their relevance to fire/explosion risk. Many toxic components have been identified but HF and CO are the most recorded. It is shown a single 18650 cell can lead to a contaminated volume of $400 \, m^3$ and toxicity remains an issue at all SOC.

No standard testing procedure is used within the academic literature, unlike, for example, the use of accelerated rate calorimetry to determine thermal hazards of cells. Many authors use custom equipment with different gas monitoring setups, open/closed systems and systems of different enclosure sizes. This increases the difficulty in comparing results from different research groups and should be a consideration of the community to resolve.

The above raises the following questions which we aim to answer in our analysis. How does the chemistry, form, capacity and SOC impact the:

- specific gas production?
- toxicity (specifically CO and HF production)?
- gas composition?

3. Methods

To allow for a definitive analysis of the off-gas behaviour from LIB TR, a comprehensive literature search of the topic needs to be ensured. To do so, the literature search was conducted with the keywords "lithium-ion" or "Li-ion" or "LIB" and "cell" or "battery" or "EV" and "abuse" or "thermal runaway" or "fire" and "off-gas" or "venting" or "gas analysis". From this, 60 papers [1–5,7,8,23–43,46,48–50,56,58–61,75–77,80,82,88–95,97–104] were deemed as appropriate and used to collate data on scale of battery (from cell to EV), form of cell, chemistry of cell, elemental ratio of cell chemistry, abuse type, cell capacity, test capacity or energy rating, SOC, nominal voltage (of cell), gas testing equipment, rate of $CO_2/CO/HF$, duration of test, total volume or mass of off-gas and quantities of individual components (g, mmol or litres) or percentage ratios. Conversion between units (g, mmol or litres) was done assuming standard temperature and pressure. The compiled data is supplied in full in the Supplementary Data. The literature data is then used to understand the influence of cell chemistry, cell type, battery scale, SOC and atmosphere on off-gas characteristics. The method of gas analysis and abuse type are recorded but not analysed for effect on LIB off-gas, and neither is the equipment setup (particularly closed versus open), but comments are made in the discussions.

4. Results and discussion — analysis of Li-ion off-gas emissions from literature

4.1. Bibliography summary

Given the literature collated, it can be seen from Fig. 2 that over the past ten years there has generally been an increasing number of papers published each year investigating the LIB off-gas, which to date leads to a total of 60 papers used in this analysis. Further subdivision of the number of papers that study specific form, cell type and chemistry can be found in the supplementary material. Within these papers most (53) focus on cell level studies while only 12 investigate larger scales including only 2 studying EV packs, see Fig. S1(a). Note that the number of papers to study specific categories can sum to more than the total (60) papers analysed as some papers may study more than one category, i.e. multiple cell forms or chemistries.
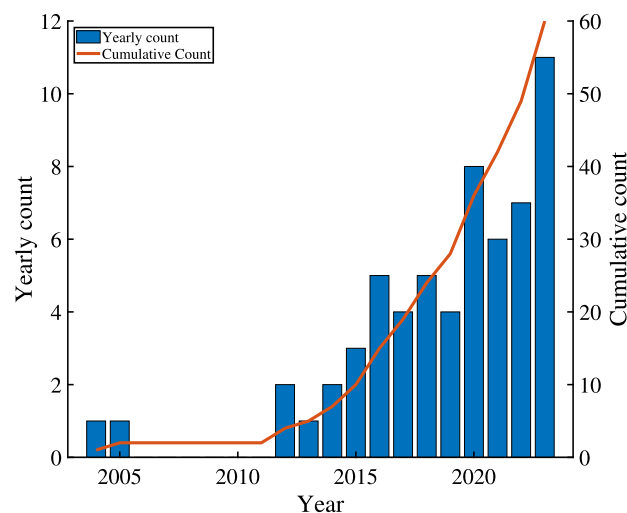

Fig. 2. Bibliography summary on a yearly basis, number of publications studying LIB TR off-gas.

At the cell level there are an approximately equal number of papers studying the off-gas of cylindrical, pouch and prismatic cells, see Fig. S1(b). Regarding chemistry, 31, 20 and 13 papers investigate NMC, LFP and LCO respectively, see Fig. S1(c). Further, NMC has mostly been studied in the past 4 years (2020–2023) with less studies on LFP in the last 3 years (2021–2023) than the 2 prior (2019–2020). Within the NMC chemistry a significant number of studies (over the entire date range) do not report the elemental ratios of nickel, manganese and cobalt, see Fig. S1(c). However, since 2020 there has been an increase in the number of studies reporting the elemental ratios, with the majority now being reported. In the last 2 years the most studied have been NMC811 and NMC622.

4.2. Total gas volume emitted

The first step in quantifying the hazard of LIB TR off-gas is determining the volume emitted. Fig. 3 presents the total amount of off-gas emitted at 100% SOC across a range of battery capacity scales, from cell to EV. This shows that as battery capacity increases so does the total amount of off-gas production. Further, it can be seen that below $0.02 \, kW \, h$ the results are mainly comprised of cylindrical cells with NCA, LFP and LCO chemistries. Above this, up to $1 \, kW \, h$, the results are of prismatic and pouch cells, predominantly of NMC chemistry. For a more detailed view of these regions see Fig. S2 in the supplementary material. This highlights the lack of analysis of high capacity ($10 \, Ah$ to $100 \, Ah$) LFP pouch/prismatic cells. Interestingly, the results below $0.02 \, kW \, h$ show more variation than above this value. This suggests that cylindrical cells may have a larger range of off-gas production than pouch or prismatic cells.

Further to the absolute volume of off-gas, Fig. 3(b) presents the specific volume of off-gas relative to the LIB capacity. This reveals that there is no correlation between capacity and the specific off-gas volume. To assess this further, and to determine the relative variability of each cell type, Fig. 4 presents a box plot of the specific off-gas generation for each cell type. For all box plots in this work the shaded box is the inter quartile range (IQR), the horizontal line within the shaded box is the median and the whiskers are the minimum and maximum values (excluding outliers). Individual data points are displayed as red scatter points while points more than 1.5IQR from the shaded box are deemed as outliers. From this it can be seen that more gas is typically produced by prismatic cells (where median values are 598 L/kWh - air, 573 L/kWh - inert) and pouch cells (502 L/kWh - air, 408 L/kWh - inert) than cylindrical cells (156 L/kWh - air, 157 L/kWh - inert). This
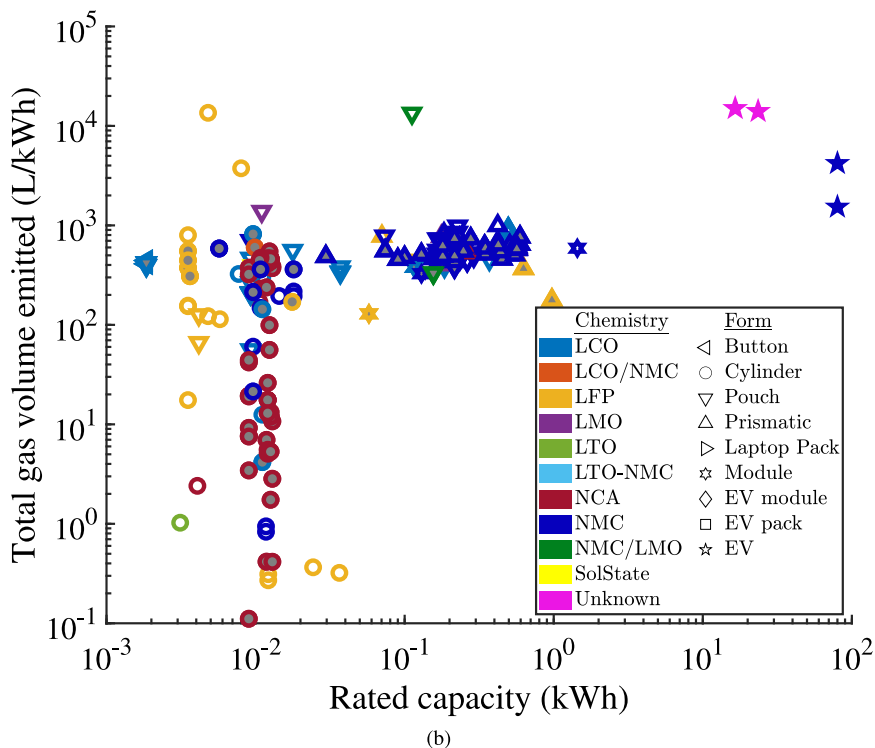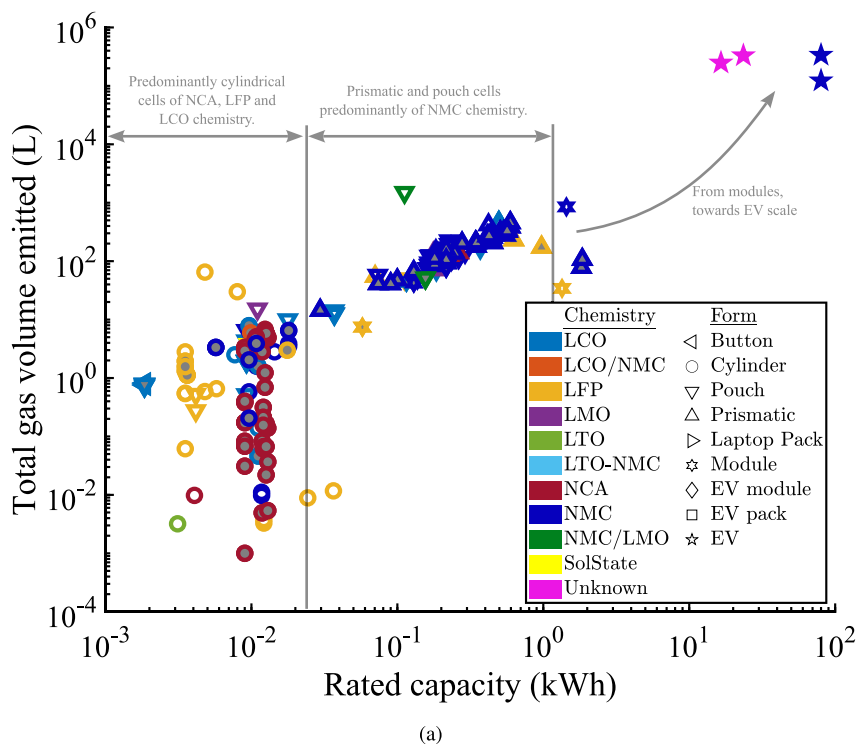
(a)

(b)

Fig. 3. Total amount of gas emitted from LIB failure given rated battery capacity for batteries at 100% SOC considering all chemistries and form factors (a) absolute values, (b) specific values. Unfilled points are from tests conducted in air, grey filled points are from tests conducted in an inert atmosphere, coloured filled points are of an unknown SOC but assume 100% SOC for this plot.

is similar to the behaviour shown by Rappsilber et al. [19]; however, here there are 93, 56 and 72 data points used within the cylindrical, pouch and prismatic cells types, respectively, compared to 12, 5 and 3 in Ref. [19]. Furthermore, here the data is split by atmosphere — air or inert. For cylindrical and prismatic cells the medians are similar for each atmosphere, while for pouch cells the inert atmosphere leads to less off-gas production. The variation in off-gas production is similar for

each cell type in air, while in an inert atmosphere pouch and prismatic cells have less variation than cylindrical.

Although Fig. 4 shows prismatic and pouch cells to produce more off-gas than cylindrical cells, Fig. 3 shows that for the collated data these cell types are predominantly NMC. For clarity, Table S1 shows the number of data points of each chemistry for each cell type in Fig. 4. From this it can be seen that the prismatic, pouch and cylindrical
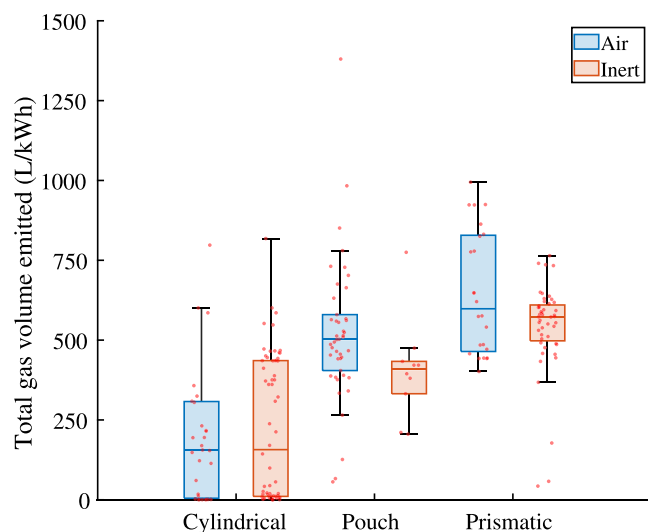
Fig. 4. Considering cell results only, the total amount of off-gas emitted from LIB failure at 100% SOC grouped by cell type. (The number of values in each category are *Form [Air, Inert]*: Cylindrical [31, 62], Pouch [46,10] and Prismatic [24, 48].).
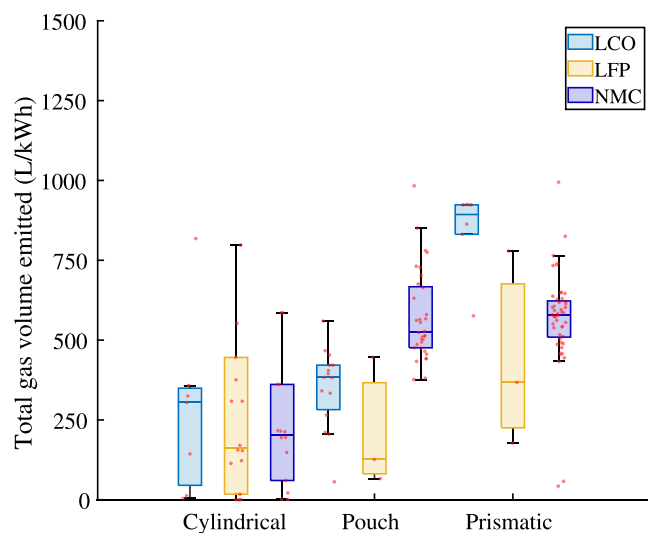

Fig. 6. Considering cell results only, the total amount of off-gas emitted from LIB failure at 100% SOC grouped by cell chemistry. (The number of values in each category are *Form [Air, Inert]*: LCO [20, 10], LFP [17, 7], NCA [3, 51] and NMC [44, 52].).

Fig. 5. Considering cell results for LCO, LFP and NMC chemistries, the total amount of off-gas emitted from LIB failure at 100% SOC grouped by cell type (both in air and an inert atmosphere). (The number of values in each category are *Form [LCO, LFP, NMC]*: Cylindrical [7, 18, 14], Pouch [15, 3, 33] and Prismatic [6, 3, 41].).

group data points are 68%, 59% and 15% NMC chemistry. As the literature has suggested (see Section 2.1), NMC produces more off-gas than other chemistries. Hence, it is necessary to analyse the off-gas volume regarding cell type and chemistry to determine if prismatic cells produce more off-gas due to their form or due to the data being mostly NMC. This is presented in Fig. 5 for LCO, LFP and NMC chemistries as the other chemistries lack data to compare across all cell types (see Table S1). Note that Fig. S3 shows outlines not present in Fig. 5 due to the scale used to improve clarity.

Fig. 5 shows that LCO prismatic and pouch cells have a greater generation of off-gas than cylindrical cells (where median values are 893 L/kWh, 383 L/kWh, 303 L/kWh - prismatic, pouch, cylindrical respectively). This is similar for the NMC chemistry, however pouch and prismatic cells produce similar amounts of off-gas (579 L/kWh, 524 L/kWh, 203 L/kWh - prismatic, pouch, cylindrical respectively). For the LFP chemistry, the increase in off-gas generation of prismatic
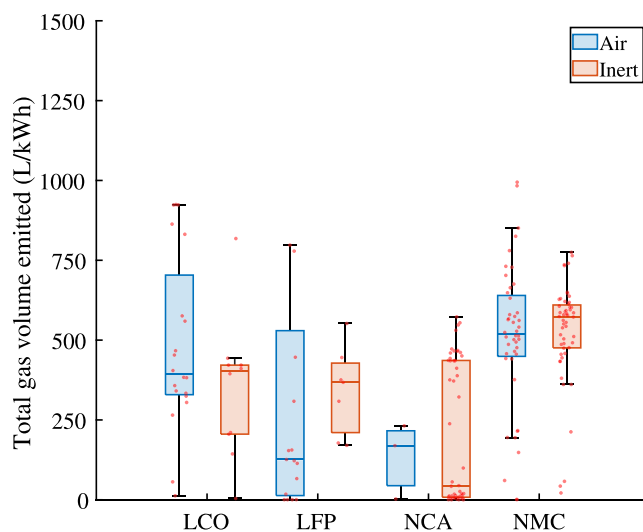
cells relative to cylindrical (368 L/kWh - prismatic, 163 L/kWh - cylindrical) is less than the LCO and NMC chemistries. Also LFP pouch cells produce an off-gas volume (126 L/kWh) similar to cylindrical cells. Overall, from Figs. 5 and 6, it is likely that more off-gas is generated by prismatic, than pouch and finally cylindrical cells.

To corroborate the literature statement that NMC produces more off-gas than other chemistries (see Section 2.1), Fig. 6 presents the specific volume of off-gas production for LCO, LFP, NCA and NMC chemistries. Note that Fig. S4 shows outliers not present in Fig. 6 due to the scale used to improve clarity. Other chemistries have been recorded, see the compiled CSV data table in the supplementary materials, but are not presented due to lack of sufficient data. Fig. 6 shows, from the median of the data, that the NMC chemistry does produce more off-gas than other chemistries (LCO: 394 L/kWh, 403 L/kWh; LFP 126 L/kWh, 368 L/kWh; NCA 169 L/kWh, 44 L/kWh; NMC 519 L/kWh, 573 L/kWh - air and inert respectively). In an inert atmosphere it is likely that NMC cells produce more gas than other chemistries. However, in air there is a chance that NMC cells will produce the same amount of off-gas as LCO and LFP. Comparison to NCA chemistry in air is omitted due to the being only 3 data points for this set. Furthermore, given the available data, there is no definitive difference in gas volume production between the two atmospheres.

While Fig. 6 presents data at 100% SOC, Fig. 7 presents the off-gas volume for LCO, LFP and NMC chemistries over various SOC. This data is mostly of cells as only 2 data point in the 100% SOC group are for any other battery scale. Fig. S5 presents similar results for the additional chemistries LMO and NCA, but is not included in the main analysis due to the lack of data at lower SOC. From Fig. 7 it can be seen that there is a strong tendency for increased gas production at higher SOC for LCO and NMC chemistries, while for LFP the increase is less steep. Also, both LFP and LCO show that there is a possibility for more gas to be produced at 0% SOC than at 25% SOC. The median values of off-gas production are similar between LCO and NMC chemistries across SOC. While for LFP the median values are similar to LCO and NMC at SOC 25% and lower, but at higher SOC the LFP chemistry has a lower median. However, the LFP chemistry shows a large variation in off-gas volume at each SOC. As such, it is possible for them to produce as much off-gas as LCO and NMC at all SOC. Further, due to the variation in the NMC chemistry it is possible that they themselves could produce similar or more off-gas at lower SOC than at higher SOC. It should be noted that there are significantly less data points at SOC less than 100%, hence this should be a focus of the academic community.
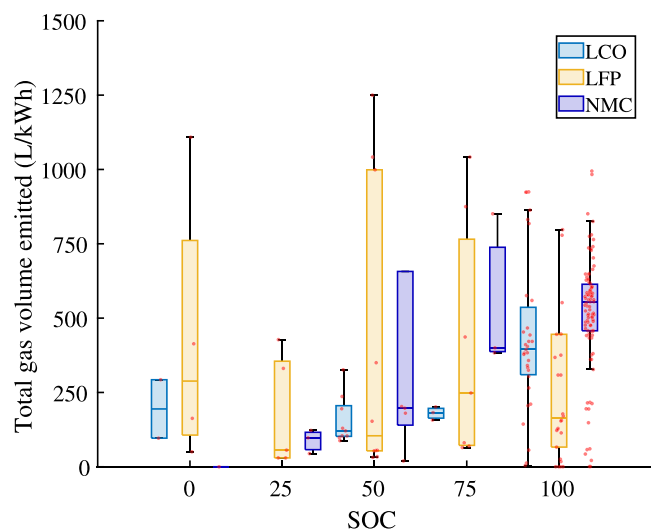
Fig. 7. The specific total amount of off-gas emitted from LIB failure at various SOC for air and inert atmosphere. (The number of values in each category are *SOC % [LCO, LFP, NMC]*: 0% [2, 4, 1], 25% [0, 5, 3], 50% [9, 10, 5], 75% [3, 7, 3] and 100% [31, 26, 98]).

For a clearer view of the median trends see Fig S6 which also presenting intermediate SOC as well as overcharge data. However, these additional SOC points typically only consist of one data entry, but from Fig S6 it can be seen there is a typical trend for LCO, LFP and NMC chemistries on overcharge to produce more off-gas than at 100% SOC. For the NCA chemistry there is negligible increase with overcharge.

It is of interest to determine if the severity of TR and off-gas production volume has changed over time with cell chemistry developments, i.e. with new additives or electrolyte compositions. Analysing the compiled data shows that on the whole there is no change in total specific off-gas production with time, see Fig. S7. LCO and NCA chemistries show an increase in the latter few years, but considering cell capacity, form, atmosphere and abuse type, no variables are determined to be influential. Hence, unknown cell material differences, differences in experimental setup or natural variation may be the cause.

4.3. Toxicity - HF and CO emissions

The total emission of HF and maximum emission rate is presented in Fig. 8, both of which increase with battery capacity. From this, it can be seen that the smallest cells release 0.01 g to 1 g of HF while larger cells release 0.1 g to 100 g and packs/EVs release kilogrammes of HF. The majority of cells studied are of LFP chemistry while NMC cells and EVs are studied to a lesser extent. The emission rates are less reported range from 10^{-4} g/s to 1 g/s from cell to EV scale (excluding HF release from air-conditioning).

The average HF emissions for LFP and NMC tests over various SOC is presented in Fig. 9 (note most of this data is related to cells as there is only one non-cell data point in the 100% SOC category). From this it is clear that the LFP chemistry typically releases over ten times more HF than the NMC chemistry normalised against battery capacity (50 g/kWh to 100 g/kWh for LFP vs <10 g/kWh for NMC). LFP cells show a slight downward trend in emissions as SOC increases (100 g/kWh at 0% SOC to 50 g/kWh at 100% SOC), due to higher TR temperatures reached (see Section 2.3), but NMC do not. However, due to the large variation in results there is little certainty that higher SOC will have lower emissions than lower SOC.

Note that there is limited data for LMO, NCA and LCO cells, although at 100% SOC LMO, NCA and NMC/LMO cells emit approximately 60 g/kWh, while LCO emit 15 g/kWh. LMO cells show a negative trend with SOC, while LCO do not show any trend.

Fig. 10 shows the maximum HF emission rate given SOC normalised against battery capacity. This shows that NMC cells have an increased rate with SOC (0.1 g/(s kWh) to 0.7 g/(s kWh)) while LFP do not. It also shows NMC cells have a much greater rate at larger SOC (0.7 g/(s kWh) for NMC vs 0.1 g/(s kWh) for LFP). This is attributed to the greater severity and strong SOC dependence of NMC failure.

The total emission of CO and maximum emission rate is presented in Fig. 11, showing both increase with battery capacity (most of the data is from cells, only four and two points at 25% and 100% SOC are not cells for LFP). Comparing Fig. 8 and Fig. 11 it can be seen that there is approximately an order of magnitude more CO emitted than HF given battery capacity, with rates also larger. A more detailed analysis of the CO emissions with SOC shows that at 100% SOC batteries with an NMC chemistry emit 10 times more CO specific to battery capacity than the LFP chemistry (172 g/kWh for NMC vs 19 g/kWh for LFP). Further, the CO emission of NMC batteries is two orders of magnitude greater than HF emissions, while for LFP the emissions are on the same order of magnitude. NMC batteries show a tendency to release more CO with increased SOC (10 g/kWh to 172 g/kWh for 25% to 100% SOC), while LFP batteries show a slight overall downward trend but there are unexpectedly low values at 25% and 75% SOC. This discussion has so far considered air and inert atmosphere data together. Fig S8 compares the results for LFP and NMC chemistries under both atmospheres and shows no statistical difference. As with the total volume (see Section 4.2), assuming composition is independent of atmosphere, the increase in total CO amount in NMC cells is both due to the chemistry and cell form leading to greater gas production.

4.4. Gas composition

A comparison of gas composition for each major chemistry over various SOC would be ideal. However, due to limited data only meaningful comparisons can be made for LFP and NMC at 100% and 50% SOC in air and 100% in an inert atmosphere. Results from tests in an inert atmosphere are considered as they simulate a scenario where oxygen is limited, such as in a sealed pack. Therefore, the gas composition before combustion can be determined, allowing for a truer assessment of off-gas hazards. Results for LFP and NMC in air at 100% SOC are presented in Fig. 13, other LFP and NMC results along with limited data for LCO and NCA is presented in Fig. S9 and Fig. S10. In these figures, *electrolytes* (Elect.) contains DMC, DEC, EMC and EC; *organic compounds* (org. comp.) contains ethanol, methanol, DME and methyl formate; *F containing compounds* (F comp.) is anything containing fluorine (including HF); and *other* is anything not listed in the graph or these categories. Note, due to a lack of compositional analysis tests in the literature concerning HF in LIB off-gas, only minimal data is available on HF as a fraction of the total gas. As such, there are fewer data points related to HF in the compositional analysis here than in the analysis of absolute HF production (Section 4.3).

For LFP at 100% in air (see Fig. 13), on average, the major component of the off-gas is H_2 (36%), then CO_2 (25%), CO (12%) and THC (11%). For NMC in similar conditions CO_2 (36%) is the major component, then CO (25%), H_2 (20%) and THC (12%). The greater CO and CO_2 generation by NMC is attributed to the tendency of NMC to lead to fires in air. Note, in previous works, non of the studies in air were set-up to record the emissions of electrolyte. Furthermore, there is no correlation of composition (percentage of species CO, CO_2, H_2 or THC) with battery capacity, see Fig. S11.

Consider 50% SOC in air for LFP and NMC (see Fig. S9(a)) there is no meaningful difference in results when compared with 100% SOC (Fig. 13). Comparing atmospheres (see Fig. S9(b)), we see that there is a greater variation in CO_2 percentage for LFP and greater H_2 generation than in Fig. 13. These results also show that electrolyte vapour is emitted to a small percentage, as well as O_2 to a lesser extent. From Fig. 13 it can be seen that H_2 is a significant flammability/explosion concern as it is typically present in a greater proportion than the THC content.
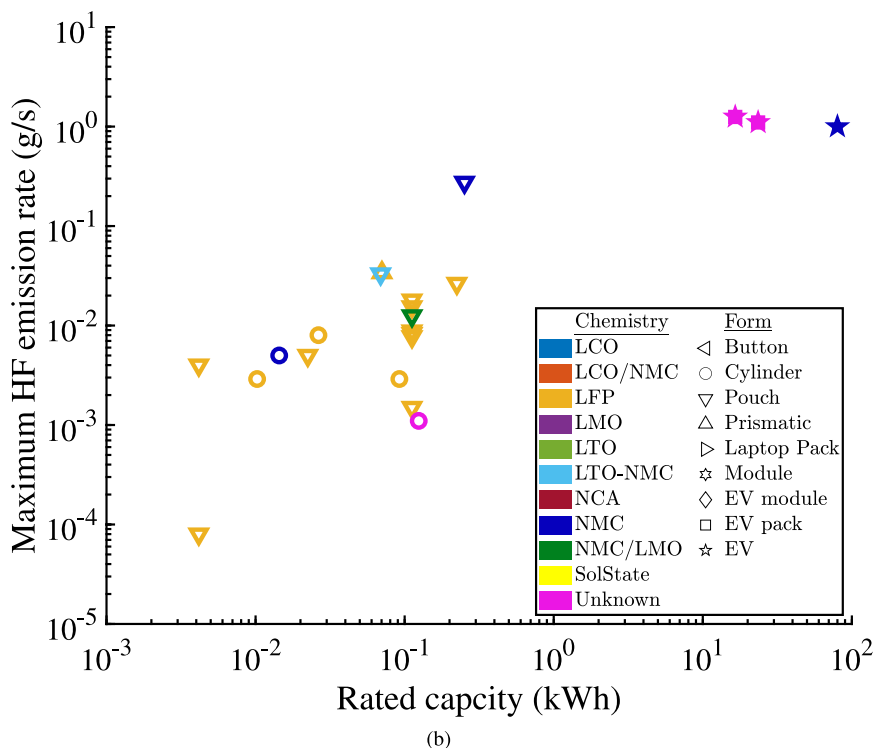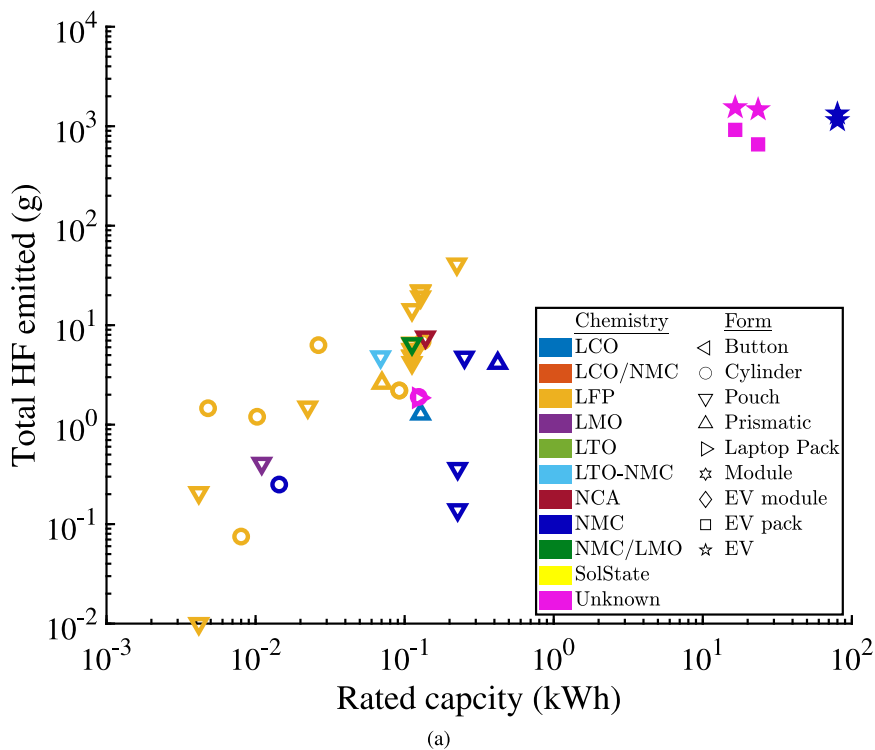
Fig. 8. HF emissions from LIB failure given rated battery capacity for batteries at 100% SOC considering all chemistries and form factors (a) total mass emitted, (b) maximum rate of emissions. Unfilled points are from tests conducted in air, grey filled points are from tests conducted in an inert atmosphere, coloured filled points are of an unknown SOC but assume 100% SOC for this plot.

It is also present in greater quantities for the LFP chemistry. The risk of H_2 content and also the role of cell chemistry on flammability is further discussed in Section 4.5.

As the emissions of gas species are interdependent, correlation plots are presented to understand the relation between the production of

each gas, see Fig. S12 and Fig. S13. However, there is no consistent behaviour between chemistries or atmospheric conditions. This is attributed to the unpredictability of combustion occurrence, and the effect the test set-up has on the availability of oxygen to promote combustion i.e. if the system is open or closed and the working volume.
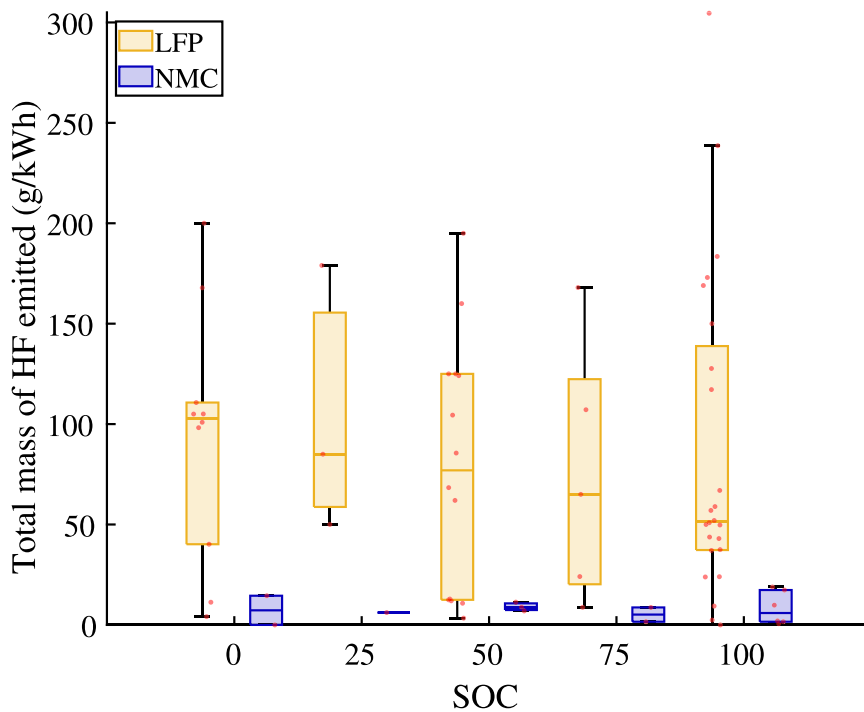
(a)
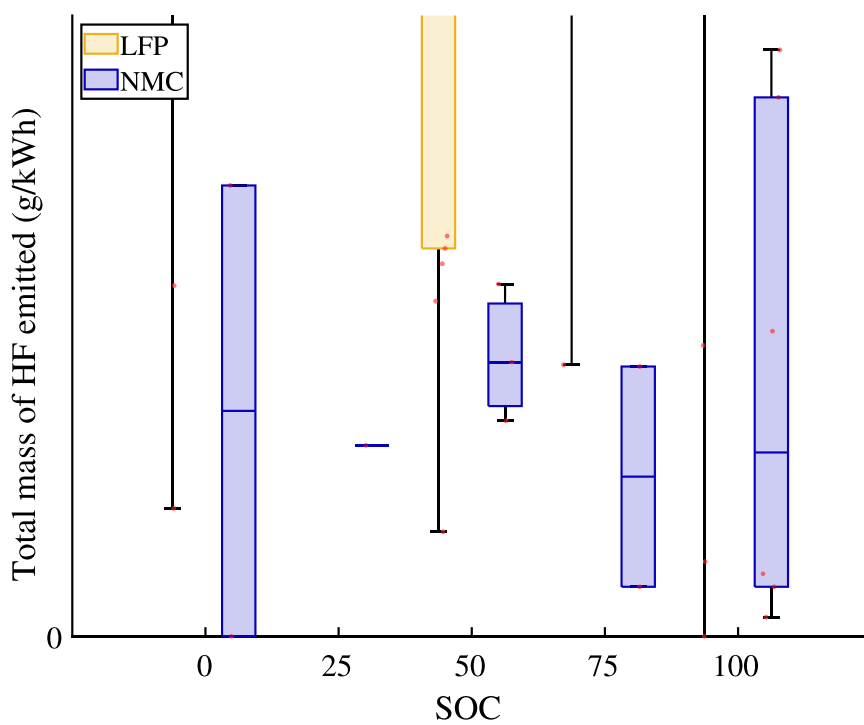
(b)

Fig. 9. (a) The specific total mass of HF emitted from LIB failure at various SOC in air, (b) enlargement of NMC data. (The number of values in each category are *SOC % [LFP, NMC]*: 0% [10, 2], 25% [3, 1], 50% [14, 3], 75% [5, 2] and 100% [24, 6].)

4.5. Discussion and recommendations

From Section 4.1 it can be noted that there is a lack of studies on the off-gassing of modules and packs. Addressing this in the academic community is important to understand how the behaviour of off-gassing and its composition changes with scale so that the change in hazards with scale can be properly assessed. However, the literature does study cell form evenly between the three main types (cylindrical, pouch and prismatic) and focuses on the two chemistries mainly used in automotive sector NMC and LFP. As such the literature is useful for the industrial community. Although the elemental ratio of NMC cells is reported more in recent years, a third of papers still do not.
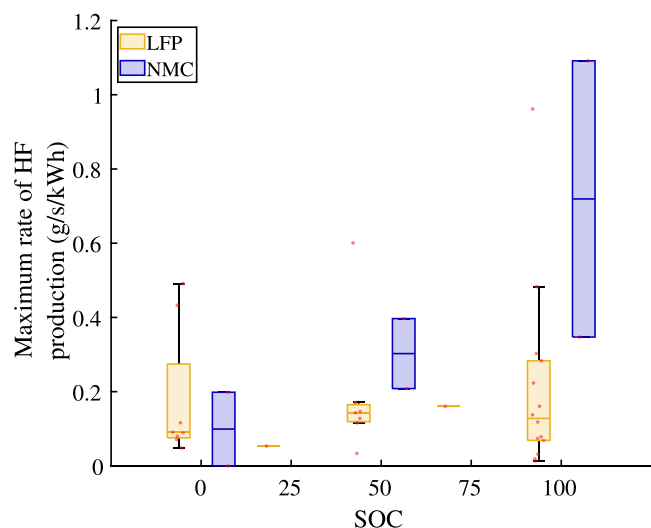
Fig. 10. The specific maximum rate of HF production from LIB failure at various SOC in air. (The number of values in each category are *SOC % [LFP, NMC]*: 0% [8, 2], 25% [1, 0], 50% [7, 2], 75% [1, 0] and 100% [14, 2].).

Table 3
Theoretical contaminated volume calculated from median HF and CO emissions for a 0.01 kWh battery.

Emissions at 100% SOC (g/kWh)		
Component i	NMC	LFP
CO	172	19
HF	6	52
Emissions at 0% SOC (g/kWh)		
Component i	NMC	LFP
CO	10[a]	34
HF	7	102
Contaminated Volume (m³)		
SOC	NMC	LFP
100%	115	355
0%	51	695

[a] Estimated from data at 25% SOC.

Hence, the academic community should encourage reporting of this to better understand the role of chemical composition of NMC on off-gas behaviour.

From the analysis in Section 4.2 it is clear that there is a strong positive correlation between off-gas volume and battery capacity across the entire range from Wh to kWh. However, the amount of gas produced specific to battery capacity is independent of battery capacity. NMC batteries do tend to produce more gas than other chemistries when considering all battery types. In general prismatic cells tend to produce more off-gas than pouch followed by cylindrical cells, even when considering chemistry. This could be caused by the large form factor having lower heat loss per unit volume leading to higher temperatures and increased decomposition. When considering separate cell forms, cylindrical LFP and NMC cells have similar medians and ranges, while LCO have a great median. For prismatic cell NMC produce less off-gas than LCO. However, there is limited data for cylindrical and prismatic LCO cells and also pouch and prismatic LFP cells which hinders comparison. Cylindrical cells and LFP chemistry show a slight tendency for greater variation in gas volume production.

As LFP are widely used in the automotive sector, more analysis of LFP pouch and prismatic cells at the scale of 10–100 Ah is crucial for hazard assessment between NMC and LFP batteries. Also, as the literature (see Section 2.6) has shown, it is difficult to scale cell TR behaviour to stack/module/pack TR behaviour. As such, comparisons of LFP and NMC batteries of a given capacity constructed of different cell forms need to be rigorously conducted to determine if there is any real difference in TR hazards, including gas hazards.

The amount of gas produced in air is not consistently more or less than that generated in an inert atmosphere, so the effect of the atmosphere on off-gas volume production is considered negligible. As is commonly suggested in the literature (Section 2.1), larger SOC typically leads to greater off-gas volumes while NMC LIBs generate more gas than LFP over all SOC. The variation within the data means that given a chemistry, a higher SOC may not lead to more gas, while LFP LIBs may produce as much as NMC LIBs. However, at SOC other than 100% and at overcharge there is significantly less data, typically less than 10 data points and only 1 for stages of overcharge (for each chemistry). Overcharge is a typical area of concern as it can occur undetected within battery operation. Hence it is critical to risk assessments to understand how the off-gas generation evolves with overcharge and should be a focus of the research community.

The toxic component analysis in Section 4.3 shows HF release from LFP cells is greater than from NMC over various SOC, with a median in the range of 60 g/kWh to 100 g/kWh for LFP versus less than 10 g/kWh for NMC. However, the rate of HF release is greater for NMC cells than LFP cells at higher SOC, due to the increased severity of TR of NMC versus LFP. LFP show the trend of less HF production at higher SOC due to increased temperature of TR, while NMC show no trend due to relatively high TR temperatures at all SOC. The release of CO is greater for NMC cells compared to LFP cells. Over 0% to 100% SOC the release is 11 g/kWh to 172 g/kWh for NMC compared to 34 g/kWh to 19 g/kWh for LFP. Although several studies have investigated the absolute HF production, few have done so as a fraction of the overall composition of the off-gas (see Section 4.4). This should be a consideration for the academic community to determine if there are any correlations of the fraction of HF to other off-gas species to complement the correlations of SOC and cell chemistry analysed in this work.

As the HF and CO production vary greatly with chemistry and SOC, the overall toxicity hazard has to be assessed considering the total amounts of all toxic components. This can be done by calculating the theoretical contaminated volume (m³) according to Eq. (1) [50]. Where m is the mass (mg) of the toxic component i which has an exposure limit value EL (mg/m³). The short term exposure limits (in the UK) for HF and CO are 1.5 mg/m³ and 23 mg/m³, respectively [54]. With this and the median HF and CO emissions for NMC and LFP at 0% and 100% SOC (see Figs. 9 and 12), Table 3 presents the calculated contaminated volume assuming a 0.01 kWh battery (this is the scale of a single cylindrical cell). Note median values are used as there are limited sources that reports both CO and HF emissions together for all four cases.

$$V_{contaminated} = \sum_{i=1}^{n} \frac{m_i}{EL_i} \tag{1}$$

From Table 3 it is shown that LFP batteries are significantly more toxic than NMC batteries when considering both major toxic components, especially at 0% SOC. This is due to the very low exposure limit of HF and the higher emissions of HF by LFP batteries. However, LFP batteries are nearly half has hazardous at 100% SOC than at 0% SOC as both HF and CO reduce at higher SOC. In comparison, NMC batteries are over twice as toxic at 100% SOC than 0% due to the large increase in CO emissions. Further, the lowest emissions from a single cell (approximately 0.01 kWh) are enough to full a single car garage or 20 ft shipping container. But at a large cell or module scale (where simultaneous burning is possible) contaminated volumes would be 10 and 100 times greater respectively. From this, LFP batteries can be said to be more toxic than NMC (in absolute terms) even though they produce on average less off-gas overall. However, the suffocation (from CO_2 emissions) and flammability hazards have to also be considered, discussed below.
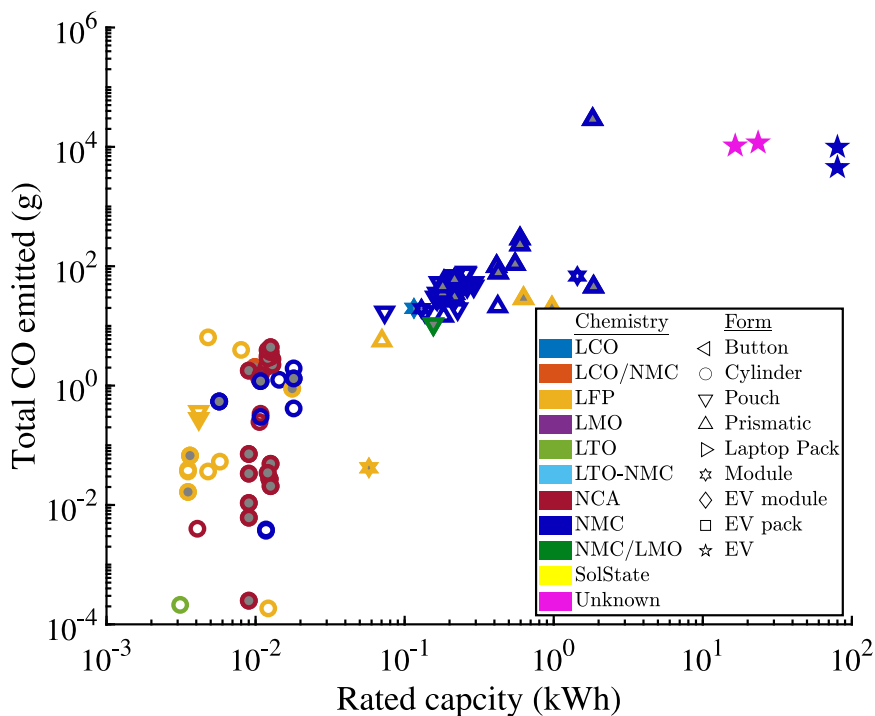
(a)
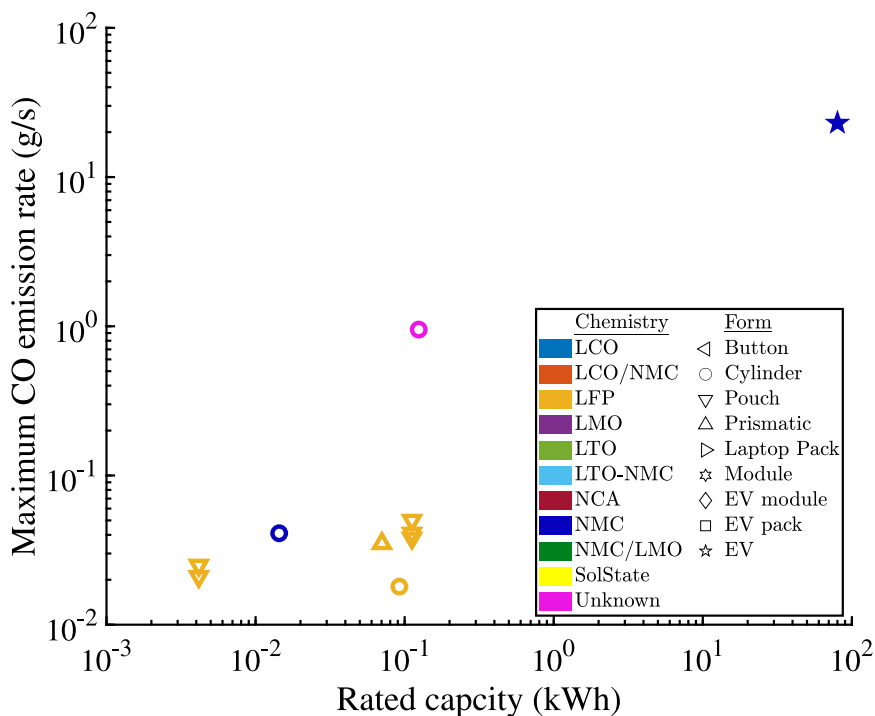
(b)

**Fig. 11.** CO emissions from LIB failure given rated battery capacity for batteries at 100% SOC considering all chemistries and form factors (a) total mass emitted, (b) maximum rate of emissions. Unfilled points are from tests conducted in air, grey filled points are from tests conducted in an inert atmosphere, coloured filled points are of an unknown SOC but assume 100% SOC for this plot.
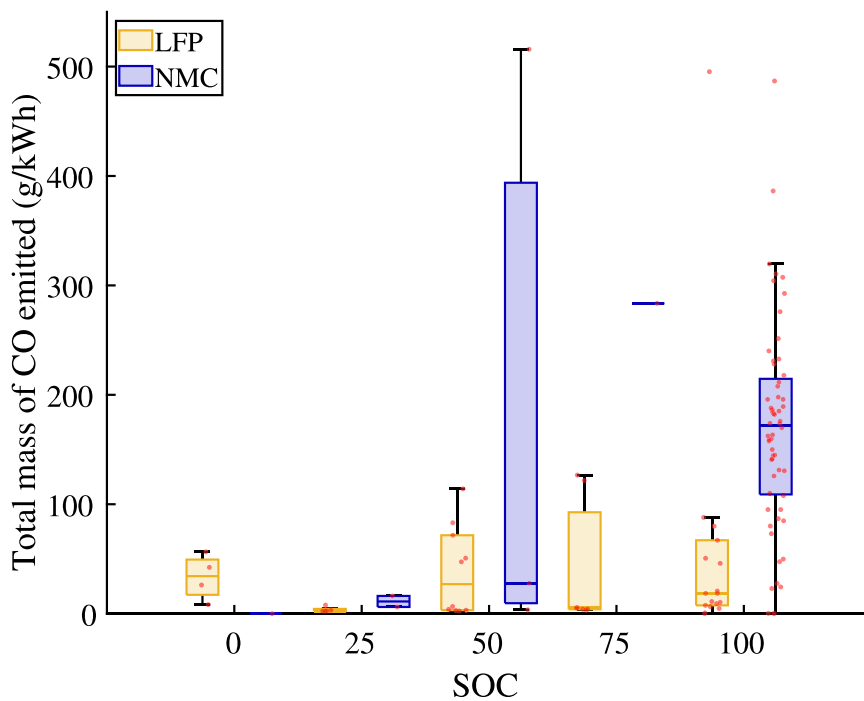
(a)
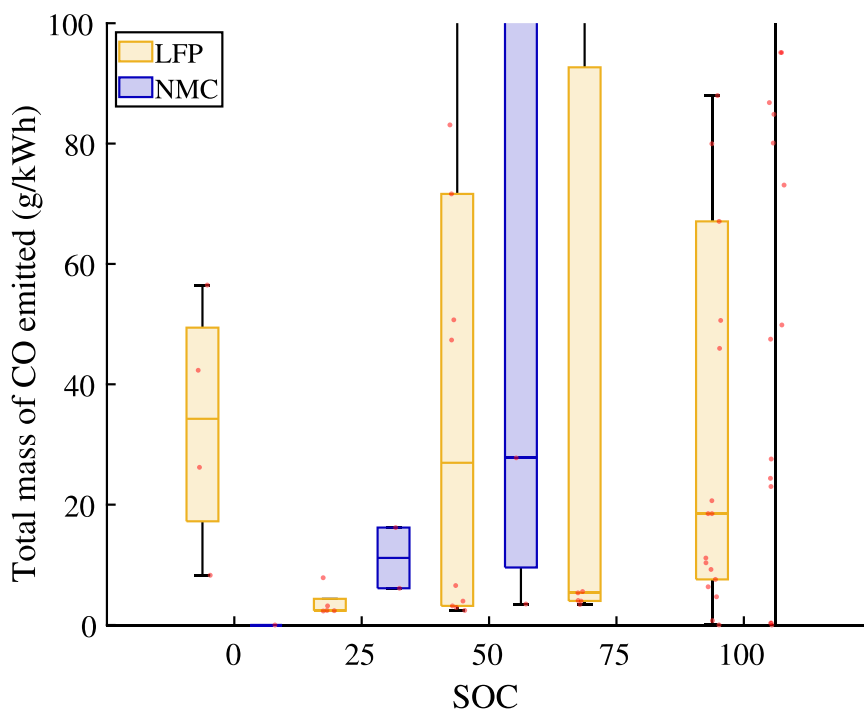
(b)

Fig. 12. (a) The specific total mass of CO emitted from LIB failure at various SOC in air, (b) enlargement of LFP data. (The number of values in each category are *SOC % [LFP, NMC]*: 0% [4, 1], 25% [5, 2], 50% [10, 3], 75% [7, 1] and 100% [18, 60].)

From the gas composition results of Section 4.4 it is shown there is a lack of data quantifying electrolyte solvent emissions, especially in air, as experiments are not set-up to detect it. This should be address as the electrolyte vapour is considered to be a significant flammability hazard. Further, tests set up should be assessed to ensure it does not affect results, i.e open/closed system limiting combustion. From analysis of the off-gas composition, it is found that the LFP chemistry releases

more H_2 than NMC on average, while more CO is emitted by NMC with similar hydrocarbon contents in both. However, it is difficult to assess the overall flammability hazard from this data. Hence, to assess the flammability hazard of each chemistry the lower flammability limit (LFL) of the off-gas mixture is calculated. This is done according to the methods in Ref. [105] accounting for the dilution of the off-gas by the CO_2 generation. The LFL of each component (CO, H_2 and hydrocarbons
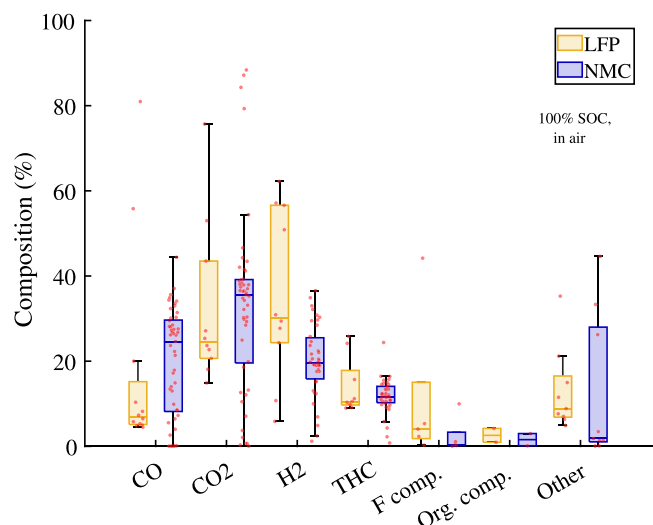
Fig. 13. Gas composition for LFP and NMC abused LIBs at 100% SOC in air. (The number of values in each category are *Gas [LFP, NMC]*: CO [12, 49], CO_2 [10, 49], H_2 [10, 39], THC [9, 39], F containing compounds [5, 5], organic compounds [2, 2] and other [9, 9].

present) are from data tables in Ref. [106]. Further detail of the LFL calculation methodology (including a table of LFL values for individual species) is given in the supplementary material.

Fig. 14 presents the calculated LFL. It can be seen that the LFP chemistry has a lower LFL (6.2%) compared to NMC (7.9% to 9.2%). This is attributed to LFP having a lower fraction of CO (which has a large LFL) and CO_2 (which dilutes the mixture), whilst having higher H_2 fractions, compared to NMC. The large range of LFL for NMC in air is attributed to the large range in CO and CO_2 production related to the variability in combustion of the off-gas leading to in/complete combustion products. Given the median LFL (Fig. 14) and gas volumes produced (Fig. 6) in an inert atmosphere then LFP batteries would breach their LFL in a volume 18% smaller than NMC cells (calculated assuming the gas is only comprised of CO_2, CO, H_2 and hydro carbons). Hence, LFP batteries present a greater flammability hazard even though they (specifically cells) show less occurrence of flames.

As noted previously, CO_2 is not considered as a toxin, but in high quantities it presents a suffocation hazard. However, Fig. 15 shows that the contaminated volume from a 0.01 kWh battery (where the short term exposure limit of CO_2 is 27 400 mg/m^3) is minimal. Even at the 1 kWh scale the hazardous volume would still be less than 10 m^3, so the suffocation hazard is low relative to the toxicity hazard.

As noted above, LFP cells show a tendency for a lower LEL but this does not account for the presence of solvents (due to lack of available data). However, as shown by Fernandes et al. [48] up to 60% of the off-gas emission can be made up of electrolyte solvents when no venting fire occurs. This will also be true for other chemistries, however, the important factor here is that due to the lower TR temperature of LFP cells it is more likely that the vent gas is emitted without combustion. This results in a greater likelihood of vapour cloud emission and accumulation, leading to an increased risk of vapour cloud explosions for LFP batteries compared to NMC. This needs to be stressed in safety and risk assessments given the general belief that LFP cells are "safe" or "the safest" in public media [e.g.107–110]. This "safest" chemistry belief is based on typical abuse tests (overheat, penetration, etc [111]) due to LFP having lower maximum temperatures and heat generation or the absence of visible sparks and flames [112–114]. However, there are many instances of LFP-based EVs under TR and emitting vapour clouds [6,10], especially in the Chinese market where LFP dominates [115]. Additional to this is the emission of toxic substances that also present a further hazard. As such, it is unwise to categorise

the safety of a battery system based on the abuse test of cells that do not account for the explosion of the off-gas (and its toxicity) or the influence of the battery system design on failure behaviour. Therefore, there should be a focus within the battery community to provide a holistic assessment of battery safety considering stability and thermal, fire/explosion and toxicity hazards.

5. Conclusion

The off-gas from Li-ion battery TR is known to be flammable and toxic making it a serious safety concern of LIB utilisation in the rare event of catastrophic failure. As such, the off-gas generation has been widely investigated but with some contradictory findings between studies. However, no work has comprehensively analysed the available literature data to determine how the chemistry, SOC, scale/capacity and form affect gas volume production, toxicity and flammability. Hence, in this work we conducted a detailed meta-analysis of 60 papers to investigate the most influential parameters and the probable off-gas characteristics to determine what kind of battery would be least hazardous.

From the analysis, it is found that LFP and NMC batteries are the most studied, aligning with industries tendency towards theses chemistries. The amount of gas produced scales linearly with capacity, however the specific gas production (L/kWh) shows no trend with capacity. NMC LIBs produce more off-gas than other chemistries (LCO 394 L/kWh, LFP 126 L/kWh, NCA 169 L/kWh, NMC 519 L/kWh), while prismatic cells also tend to generate larger off-gas volumes (cylindrical 156 L/kWh, pouch 502 L/kWh, prismatic 598 L/kWh). Also, a larger SOC does lead to greater average specific off-gas volumes specifically for NMC and LCO batteries, however there is significant variation in results.

While NMC batteries release more gas than LFP, LFP batteries are significantly more toxic than NMC ones in absolute terms. Toxicity varies with SOC, for NMC batteries the contaminated volume doubles from 0% to 100% SOC while for LFP in halves. The composition of off-gas on average is very similar between NMC and LFP cells, but LFP batteries have greater H_2 content while NMC batteries have a greater CO content. To assess the fire hazard the LFL limit of the off-gasses is compared. The LFL for LFP and NMC are 6.2% and 7.9% (in an inert atmosphere) respectively. Given the LFL and the median off-gas volumes produced, LFP cells breach the LFL in a volume 18% smaller than NMC batteries. Hence LFP presents a greater flammability hazard even though they show less occurrence of flames in cell TR tests.

Also, from this work it is found that significant improvements in research can be made. To advance the understanding of off-gas further, for improved battery safety, it is recommended that:

1. the electrode elemental ratio and electrolyte composition of cells are reported to better compare NMC results and understand the affect of electrolytes;
2. LFP pouch and prismatic cells at the scale of 10–100 Ah to be studied to address the gap in data at this scale, so that like-for-like comparisons between high energy LFP and NMC cells can be made;
3. tests at module and pack level should be conducted to understand how the hazards scale with battery size;
4. the off-gas generation is studied at other SOC other than 100% and especially at overcharge to accurately determine how toxicity and flammability hazards vary; and
5. the experimental set up is designed to ensure the detection/quantification of common electrolyte solvents to determine when and how much is emitted as a vapour and hence determine the additional flammability hazards.

Finally, this work provides a critical resource to the battery community that can be used for the risk assessment of LIB TR fire, explosion and toxicity hazards. This is aided by supplying the compiled literature data in a raw format that is readable and editable to allow independent and ongoing analysis by interested/relevant parties.
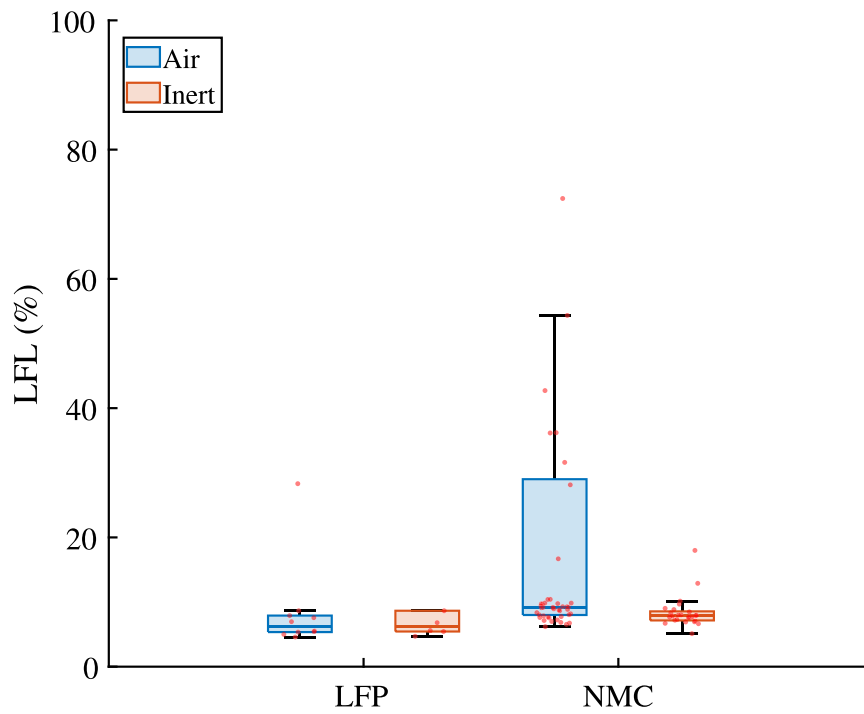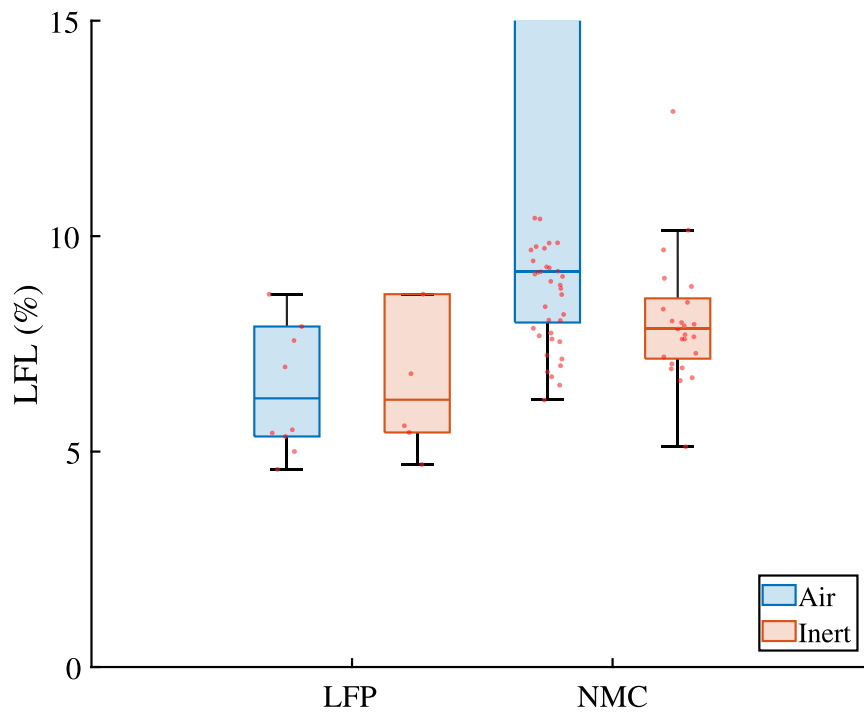
Fig. 14. (a) Calculated lower flammability limit considering CO, H_2 and hydrocarbons diluted by CO_2 (b) enlargement of data. (The number of values in each category are *Chemistry [Air, Inert]*: LFP [10, 6] and NMC [49, 25].)
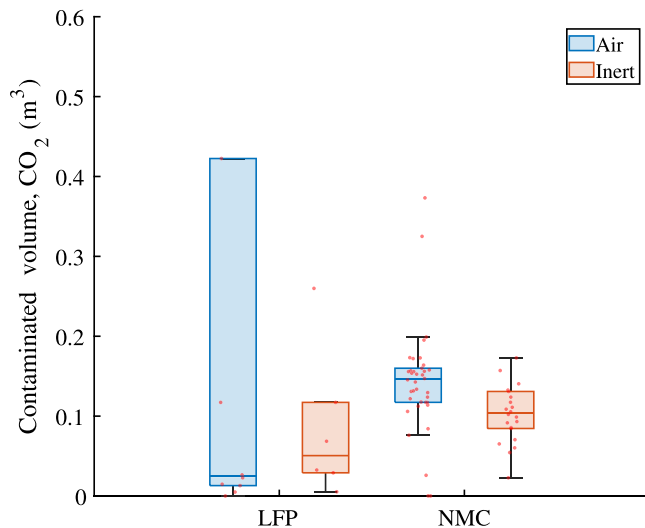
Fig. 15. Contaminated volume from CO_2 assuming 0.01 kWh battery. (The number of values in each category are *Chemistry [Air, Inert]*: LFP [10, 6] and NMC [38, 22].).

CRediT authorship contribution statement

Peter J. Bugryniec: Writing – review & editing, Writing – original draft, Visualization, Methodology, Investigation, Formal analysis, Data curation, Conceptualization. **Erik G. Resendiz:** Writing – review & editing, Data curation. **Solomon M. Nwophoke:** Writing – review & editing, Data curation. **Simran Khanna:** Writing – review & editing, Data curation. **Charles James:** Writing – review & editing, Data curation. **Solomon F. Brown:** Writing – review & editing, Supervision, Project administration, Funding acquisition, Conceptualization.

Declaration of competing interest

The authors declare that they have no known competing financial interests or personal relationships that could have appeared to influence the work reported in this paper.

Data availability

The data is made available through the CSV files available as supplementary material.

Acknowledgements

Appendix A. Supplementary data

Supplementary material related to this article can be found online at https://doi.org/10.1016/j.est.2024.111288.

References

[1] B. Truchot, F. Fouillen, S. Collet, An experimental evaluation of toxic gas emissions from vehicle fires, Fire Saf. J. 97 (2018) 111–118, http://dx.doi.org/10.1016/j.firesaf.2017.12.002, URL https://www.sciencedirect.com/science/article/pii/S0379711217307312.

[2] L.D. Mellert, U. Welte, M. Hermann, M. Kompatscher, X. Ponticq, V. Hagerbach, Electric mobility and road tunnel safety hazards of electric vehicle fires, 2018.

[3] A. Lecocq, M. Bertana, B. Truchot, G. Marlair, Comparison of the fire consequences of an electric vehicle and an internal combustion engine vehicle, in: 2. International Conference on Fires in Vehicles, FIVE 2012, SP Technical Research Institute of Sweden. Boras, Chicago, United States, 2012, pp. 183–194, URL https://ineris.hal.science/ineris-00973680.

[4] O. Willstrand, R. Bisschop, P. Blomqvist, A. Temple, J. Anderson, Toxic Gases from Fire in Electric Vehicles, Tech. Rep., RISE, 2020, URL https://www.diva-portal.org/smash/get/diva2:1522149/FULLTEXT01.pdf.

[5] P.-J. Sturm, P.F. leitner, D. Fruhwirt, S.F. Heindl, B. Kohl, O. Heger, R. Wenighofer, S. Krausbar, Brandauswirkungen von Fahrzeugenmit alternativen Antriebssystemen Tech. Rep., (Fire Effects of Vehicles with Alternative Drive Systems) 2021, [In German]. URL https://pure.tugraz.at/ws/portalfiles/portal/38365549/BRAFA_Ergebnisbericht_v1.0.pdf.

[6] P. Sun, R. Bisschop, H. Niu, X. Huang, A review of battery fires in electric vehicles, Fire Technol. 56 (4) (2020) 1361–1410, http://dx.doi.org/10.1007/s10694-019-00944-3.

[7] O. Willstrand, M. Pushp, P. Andersson, D. Brandell, Impact of different Li-ion cell test conditions on thermal runaway characteristics and gas release measurements, J. Energy Storage 68 (2023) 107785, http://dx.doi.org/10.1016/j.est.2023.107785, URL https://www.sciencedirect.com/science/article/pii/S2352152X23011829.

[8] R. Tschirschwitz, C. Bernardy, P. Wagner, T. Rappsilber, C. Liebner, S.-K. Hahn, U. Krause, Harmful effects of lithium-ion battery thermal runaway: scale-up tests from cell to second-life modules, RSC Adv. 13 (2023) 20761–20779, http://dx.doi.org/10.1039/D3RA02881J.

[9] M.B. McKinnon, S. DeCrane, S. Kerber, Four Firefighters Injured In Lithium-Ion Battery Energy Storage System Explosion - Arizona, Tech. Rep., Underwriters Laboratories Inc., UL Firefighter Safety Research Institute, Columbia, MD 21045, 2020, URL https://fsri.org/sites/default/files/2021-07/Four_Firefighters_Injured_In_Lithium_Ion_Battery_ESS_Explosion_Arizona_0.pdf.

[10] South China Morning Post, Electric bus bursts into flames, sets nearby vehicles on fire in China, 2021, video URL https://www.youtube.com/watch?v=T71cVhxG_v4.

[11] Icelandic Transport Authority Conference, 1St international symposium on fire in electric storage at sea, 2023, URL https://vimeo.com/830182462/aa852b93a7?share=copy. (Accessed 30 November 2023).

[12] H. Helgesen, S.H. ard, A.A. Langli, Study on Electrical Energy Storage for Ships: Battery Systems For Maritime Applications – Technology, Sustainability And Safety, Tech. Rep., European Maritime Safety Agency, 2020, URL https://www.emsa.europa.eu/publications/item/3895-study-on-electrical-energy-storage-for-ships.html.

[13] F. Larsson, B. Mellander, Lithium-ion batteries used in electrified vehicles – General risk assessment and construction guidelines from a fire and gas release perspective, 2017, URL https://www.diva-portal.org/smash/record.jsf?dswid=-2345&pid=diva2:1146859&c=1&searchType=SIMPLE&language=en&query=Lithium-ion+Batteries+used+in+Electrified+Vehicles+--+General+Risk+Assessment+and+Construction+Guidelines+from+a+Fire+and+Gas+Release+Perspective&af=&aq2=&aqe=&noOfRows=50&sortOrder=author_sort_asc&sortOrder2=title_sort_asc&onlyFullText=false&sf=all.

[14] M.K.H. Hsieh, M.C. Lai, H.S.N. Sim, X. Lim, S.F.D. Fok, J. Joethy, T.Y. Kong, G.J.S. Lim, Electric scooter battery detonation: A case series and review of literature, Ann. Burns Fire Disasters 34 (2021) 264–276, URL https://www.ncbi.nlm.nih.gov/pmc/articles/PMC8534310/.

[15] Electrical Saftey First, Battery breakdown why are e-scooter and e-bike batteries exploding in people's homes and what can be done about it? 2023, URL https://www.electricalsafetyfirst.org.uk/media/sgyikuwb/esf_batterybreakdown_report_2023_v7_-final.pdf. (Accessed 30 January 2024).

[16] C. Meraner, Car park fires: A review of fire incidents, progress in research and future challenges., in: Proceedings of Seventh International Conference on Fires in Vehicles, Stavanger, Norway, 2023, pp. 7–23, URL https://urn.kb.se/resolve?urn=urn:nbn:se:ri:diva-71489.

[17] A.R. Baird, E.J. Archibald, K.C. Marr, O.A. Ezekoye, Explosion hazards from lithium-ion battery vent gas, J. Power Sources 446 (2020) 227257, http://dx.doi.org/10.1016/j.jpowsour.2019.227257, URL https://www.sciencedirect.com/science/article/pii/S0378775319312509.

[18] W. Li, S. Rao, Y. Xiao, Z. Gao, Y. Chen, H. Wang, M. Ouyang, Fire boundaries of lithium-ion cell eruption gases caused by thermal runaway, iScience 24 (2021) 102401, http://dx.doi.org/10.1016/j.isci.2021.102401, URL https://www.sciencedirect.com/science/article/pii/S2589004221003692.

[19] T. Rappsilber, N. Yusfi, S. Krüger, S.-K. Hahn, T.-P. Fellinger, J. Krug von Nidda, R. Tschirschwitz, Meta-analysis of heat release and smoke gas emission during thermal runaway of lithium-ion batteries, J. Energy Storage 60 (2023) 106579, http://dx.doi.org/10.1016/j.est.2022.106579, URL https://www.sciencedirect.com/science/article/pii/S2352152X22025683.

[20] Y. Miao, P. Hynan, A. von Jouanne, A. Yokochi, Current Li-ion battery technologies in electric vehicles and opportunities for advancements, Energies 12 (6) (2019) http://dx.doi.org/10.3390/en12061074, URL https://www.mdpi.com/1996-1073/12/6/1074.

[21] W. Mrozik, M. Wise, N. Dickman, M. Ahmeid, Z. Milojevic, P. Das, S. Lambert, P. Christensen, Abuse of lithium-ion batteries: emergence, composition, and toxicity of vapour cloud, in: Book of Abstracts Nordic Fire and Safety Days, 2022, pp. 86–87, http://dx.doi.org/10.23699/sgj7-kd69, URL https://www.diva-portal.org/smash/record.jsf?pid=diva2:1657152&dswid=-8687.

[22] P. Bugryniec, Li-ion battery Thermal Runaway Flowchart, 2023, http://dx.doi.org/10.13140/RG.2.2.34249.01120.

[23] C. Essl, A.W. Golubkov, E. Gasser, M. Nachtnebel, A. Zankel, E. Ewert, A. Fuchs, Comprehensive hazard analysis of failing automotive lithium-ion batteries in overtemperature experiments, Batteries 6 (2) (2020) http://dx.doi.org/10.3390/batteries6020030, URL https://www.mdpi.com/2313-0105/6/2/30.

[24] A.W. Golubkov, D. Fuchs, J. Wagner, H. Wiltsche, C. Stangl, G. Fauler, G. Voitic, A. Thaler, V. Hacker, Thermal-runaway experiments on consumer Li-ion batteries with metal-oxide and olivin-type cathodes, RSC Adv. 4 (2014) 3633–3642, http://dx.doi.org/10.1039/C3RA45748F.

[25] A.W. Golubkov, S. Scheikl, R. Planteu, G. Voitic, H. Wiltsche, C. Stangl, G. Fauler, A. Thaler, V. Hacker, Thermal runaway of commercial 18650 Li-ion batteries with LFP and NCA cathodes – impact of state of charge and overcharge, RSC Adv. 5 (2015) 57171–57186, http://dx.doi.org/10.1039/C5RA05897J.

[26] V. Somandepalli, K. Marr, Q. Horn, Quantification of combustion hazards of thermal runaway failures in lithium-ion batteries, SAE Int. J. Altern. Powertrains 3 (1) (2014) 98–104, http://dx.doi.org/10.4271/2014-01-1857.

[27] S. Koch, A. Fill, K.P. Birke, Comprehensive gas analysis on large scale automotive lithium-ion cells in thermal runaway, J. Power Sources 398 (2018) 106–112, http://dx.doi.org/10.1016/j.jpowsour.2018.07.051, URL https://www.sciencedirect.com/science/article/pii/S0378775318307687.

[28] A.W. Golubkov, R. Planteu, P. Krohn, B. Rasch, B. Brunnsteiner, A. Thaler, V. Hacker, Thermal runaway of large automotive Li-ion batteries, RSC Adv. 8 (2018) 40172–40186, http://dx.doi.org/10.1039/C8RA06458J.

[29] D. Sturk, L. Rosell, P. Blomqvist, A. Ahlberg Tidblad, Analysis of Li-Ion battery gases vented in an inert atmosphere thermal test chamber, Batteries 5 (3) (2019) http://dx.doi.org/10.3390/batteries5030061, URL https://www.mdpi.com/2313-0105/5/3/61.

[30] K.O.A. Amano, S.-K. Hahn, N. Butt, P. Vorwerk, E. Gimadieva, R. Tschirschwitz, T. Rappsilber, U. Krause, Composition and explosibility of gas emissions from lithium-ion batteries undergoing thermal runaway, Batteries 9 (6) (2023) http://dx.doi.org/10.3390/batteries9060300, URL https://www.mdpi.com/2313-0105/9/6/300.

[31] H. Shen, H. Wang, M. Li, C. Li, Y. Zhang, Y. Li, X. Yang, X. Feng, M. Ouyang, Thermal runaway characteristics and gas composition analysis of lithium-ion batteries with different LFP and NCM cathode materials under inert atmosphere, Electronics 12 (7) (2023) http://dx.doi.org/10.3390/electronics12071603, URL https://www.mdpi.com/2079-9292/12/7/1603.

[32] X. Yang, H. Wang, M. Li, Y. Li, C. Li, Y. Zhang, S. Chen, H. Shen, F. Qian, X. Feng, M. Ouyang, Experimental study on thermal runaway behavior of lithium-ion battery and analysis of combustible limit of gas production, Batteries 8 (11) (2022) http://dx.doi.org/10.3390/batteries8110250, URL https://www.mdpi.com/2313-0105/8/11/250.

[33] D.J. Robles, J. Jeevarajan, Fire and gas characterization studies for lithium-ion cells and batteries, 2020, NASA Aerospace Battery Workshop. URL https://www.nasa.gov/sites/default/files/atoms/files/nabw20_fire_gas_char_studies_liion_cells_batt_djuarez-robles.pdf.

[34] L. Yuan, T. Dubaniewicz, I. Zlochower, R. Thomas, N. Rayyan, Experimental study on thermal runaway and vented gases of lithium-ion cells, Process Saf. Environ. Prot. 144 (2020) 186–192, http://dx.doi.org/10.1016/j.psep.2020.07.028, URL https://www.sciencedirect.com/science/article/pii/S0957582020316360.

[35] S. Hoelle, S. Scharner, S. Asanin, O. Hinrichsen, Analysis on thermal runaway behavior of prismatic lithium-ion batteries with autoclave calorimetry, J. Electrochem. Soc. 168 (12) (2021) 120515, http://dx.doi.org/10.1149/1945-7111/ac3c27.

[36] C. Essl, A.W. Golubkov, A. Fuchs, Comparing different thermal runaway triggers for two automotive lithium-ion battery cell types, J. Electrochem. Soc. 167 (13) (2020) 130542, http://dx.doi.org/10.1149/1945-7111/abbe5a.

[37] K.C. Abbott, J.E. Buston, J. Gill, S.L. Goddard, D. Howard, G. Howard, E. Read, R.C. Williams, Comprehensive gas analysis of a 21700 Li(Ni0.8Co0.1Mn0.1O2) cell using mass spectrometry, J. Power Sources 539 (2022) 231585, http://dx.doi.org/10.1016/j.jpowsour.2022.231585, URL https://www.sciencedirect.com/science/article/pii/S0378775322005882.

[38] K.O.A. Amano, S.-K. Hahn, R. Tschirschwitz, T. Rappsilber, U. Krause, An experimental investigation of thermal runaway and gas release of NMC lithium-ion pouch batteries depending on the state of charge level, Batteries 8 (5) (2022) http://dx.doi.org/10.3390/batteries8050041, URL https://www.mdpi.com/2313-0105/8/5/41.

[39] P. Liu, H. Sun, Y. Qiao, S. Sun, C. Wang, K. Jin, B. Mao, Q. Wang, Experimental study on the thermal runaway and fire behavior of LiNi0.8Co0.1Mn0.1O2 battery in open and confined spaces, Process Saf. Environ. Prot. 158 (2022) 711–726, http://dx.doi.org/10.1016/j.psep.2021.12.056, URL https://www.sciencedirect.com/science/article/pii/S0957582021007321.

[40] M. Yang, M. Rong, J. Pan, Y. Ye, A. Yang, J. Chu, H. Yuan, X. Wang, Thermal runaway behavior analysis during overheating for commercial LiFePO4 batteries under various state of charges, Appl. Therm. Eng. 230 (2023) 120816, http://dx.doi.org/10.1016/j.applthermaleng.2023.120816, URL https://www.sciencedirect.com/science/article/pii/S1359431123008451.

[41] DNV GL, Maritime Battery Safety Joint Development project: Technical Reference for Li-ion Battery Explosion Risk and Fire Suppression, Tech. Rep., 2019, URL https://safety4sea.com/wp-content/uploads/2020/01/DNV-GL-Technical-Reference-for-Li-Ion-Battery-Explosion-Risk-and-Fire-Suppresion-2020_01.pdf.

[42] P. Liu, C. Liu, K. Yang, M. Zhang, F. Gao, B. Mao, H. Li, Q. Duan, Q. Wang, Thermal runaway and fire behaviors of lithium iron phosphate battery induced by over heating, J. Energy Storage 31 (2020) 101714, http://dx.doi.org/10.1016/j.est.2020.101714, URL https://www.sciencedirect.com/science/article/pii/S2352152X20315516.

[43] L. Zhang, Q. Duan, X. Meng, K. Jin, J. Xu, J. Sun, Q. Wang, Experimental investigation on intermittent spray cooling and toxic hazards of lithium-ion battery thermal runaway, Energy Convers. Manage. 252 (2022) 115091, http://dx.doi.org/10.1016/j.enconman.2021.115091, URL https://www.sciencedirect.com/science/article/pii/S019689042101267X.

[44] U. Bergström, A. Gustafsson, lars Hägglund, C. Lejon, D. Sturk, T. Tengel, Vented Gases and Aerosol of Automotive Li-ion LFP and NMC Batteries in Humified Nitrogen under Thermal Load, Tech. Rep., 2015, URL https://www.msb.se/siteassets/dokument/publikationer/english-publications/vented-gases-and-aerosol-of-automotive-li-ion-lfp-and-nmc-batteries-in-humidified-nitrogen-under-thermal-load.pdf.

[45] A. Nedjalkov, J. Meyer, M. Köhring, A. Doering, M. Angelmahr, S. Dahle, A. Sander, A. Fischer, W. Schade, Toxic gas emissions from damaged lithium ion batteries–Analysis and safety enhancement solution, Batteries 2 (1) (2016) http://dx.doi.org/10.3390/batteries2010005, URL https://www.mdpi.com/2313-0105/2/1/5.

[46] Y. Zhang, H. Wang, W. Li, C. Li, Quantitative identification of emissions from abused prismatic Ni-rich lithium-ion batteries, eTransportation 2 (2019) 100031, http://dx.doi.org/10.1016/j.etran.2019.100031, URL https://www.sciencedirect.com/science/article/pii/S2590116819300311.

[47] Health and Safety Executive, EH40/2005 Workplace Exposure Limits, fourth ed., 2020, URL https://www.hse.gov.uk/pubns/priced/eh40.pdf ISBN 978 0 7176 6733 8.

[48] Y. Fernandes, A. Bry, S. de Persis, Identification and quantification of gases emitted during abuse tests by overcharge of a commercial Li-ion battery, J. Power Sources 389 (2018) 106–119, http://dx.doi.org/10.1016/j.jpowsour.2018.03.034, URL https://www.sciencedirect.com/science/article/pii/S0378775318302581.

[49] K. Zou, S. Lu, X. Chen, E. Gao, Y. Cao, Y. Bi, Thermal and gas characteristics of large-format LiNi0.8Co0.1Mn0.1O2 pouch power cell during thermal runaway, J. Energy Storage 39 (2021) 102609, http://dx.doi.org/10.1016/j.est.2021.102609, URL https://www.sciencedirect.com/science/article/pii/S2352152X21003510.

[50] F. Diaz, Y. Wang, R. Weyhe, B. Friedrich, Gas generation measurement and evaluation during mechanical processing and thermal treatment of spent Li-ion batteries, Waste Manag. 84 (2019) 102–111, http://dx.doi.org/10.1016/j.wasman.2018.11.029, URL https://www.sciencedirect.com/science/article/pii/S0956053X18307013.

[51] T. Shan, X. Zhu, Z. Wang, Understanding the boundary and mechanism of gas-induced explosion for lithium-ion cells: Experimental and theoretical analysis, J. Energy Chem. (2023) http://dx.doi.org/10.1016/j.jechem.2023.07.029, URL https://www.sciencedirect.com/science/article/pii/S2095495623004291.

[52] Health and Safety Executive, General hazards of Carbon Dioxide https://www.hse.gov.uk/carboncapture/carbondioxide.htm#:{~}:text=AstheconcentrationCO2,orcellarsanddisplacedOxygen.

[53] ECHA, Search for Chemicals URL https://echa.europa.eu/search-for-chemicals.

[54] IFA Institut für Arbeitsschutz der Deutschen Gesetzlichen Unfallversiicherung, GESTIS International Limit Values, 2023, URL https://limitvalue.ifa.dguv.de/.

[55] National Research Council (US) Committee on Toxicology, Emergency and continuous exposure limits for selected airborne contaminants: Volume 1, 1984, URL https://www.ncbi.nlm.nih.gov/books/NBK208285/.

[56] A.O. Said, C. Lee, S.I. Stoliarov, Experimental investigation of cascading failure in 18650 lithium ion cell arrays: Impact of cathode chemistry, J. Power Sources 446 (2020) 227347, http://dx.doi.org/10.1016/j.jpowsour.2019.227347, URL https://www.sciencedirect.com/science/article/pii/S0378775319313400.

[57] T. Maloney, Solid state battery tests, 2017, URL https://www.fire.tc.faa.gov/pdf/systems/Nov17Meeting/Maloney-1117-Solid_State_battery_tests.pdf FAA Fire Safety, Systems Meeting.

[58] Q. Zhang, J. Niu, Z. Zhao, Q. Wang, Research on the effect of thermal runaway gas components and explosion limits of lithium-ion batteries under different charge states, J. Energy Storage 45 (2022) 103759, http://dx.doi.org/10.1016/j.est.2021.103759, URL https://www.sciencedirect.com/science/article/pii/S2352152X21014328.

[59] M. Karp, J. Sica, Flammable gas analysis UN lithium battery working group, in: International Aircraft Systems Fire Protection Working Group, FAA, 2021, URL https://www.fire.tc.faa.gov/pdf/systems/April21Meeting/Karp-0421-UNGas.pdf.

[60] P. Ribière, S. Grugeon, M. Morcrette, S. Boyanov, S. Laruelle, G. Marlair, Investigation on the fire-induced hazards of Li-ion battery cells by fire calorimetry, Energy Environ. Sci. 5 (2012) 5271–5280, http://dx.doi.org/10.1039/C1EE02218K.

[61] A. Lecocq, G.G. Eshetu, S. Grugeon, N. Martin, S. Laruelle, G. Marlair, Scenario-based prediction of Li-ion batteries fire-induced toxicity, J. Power Sources 316 (2016) 197–206, http://dx.doi.org/10.1016/j.jpowsour.2016.02.090, URL https://www.sciencedirect.com/science/article/pii/S0378775316301975.

[62] T. Maloney, Lithium battery thermal runaway vent gas analysis composition and effect of combustion, 2015, URL https://fire.tc.faa.gov/pdf/systems/May15Meeting/Maloney-0515-LithiumThermalRunaway.pdf FAA presentation.

[63] L. Rong, X. Cheng, Y. Fu, Effect of States of Charge on the Burning Behaviors of Lithium ion Batteries, in: 2019 9th International Conference on Fire Science and Fire Protection Engineering, ICFSFPE, 2019, pp. 1–5, http://dx.doi.org/10.1109/ICFSFPE48751.2019.9055886, URL https://ieeexplore.ieee.org/document/9055886.

[64] Y. Peng, X. Zhou, Y. Hu, X. Ju, B. Liao, L. Yang, A new exploration of the fire behaviors of large format lithium ion battery, J. Therm. Anal. Calorim. 139 (2) (2020) 1243–1254, http://dx.doi.org/10.1007/s10973-019-08459-3.

[65] Q. Zhang, J. Niu, J. Yang, T. Liu, F. Bao, Q. Wang, In-situ explosion limit analysis and hazards research of vent gas from lithium-ion battery thermal runaway, J. Energy Storage 56 (2022) 106146, http://dx.doi.org/10.1016/j.est.2022.106146, URL https://www.sciencedirect.com/science/article/pii/S2352152X22021351.

[66] M. Yang, M. Rong, Y. Ye, A. Yang, J. Chu, H. Yuan, X. Wang, Comprehensive analysis of gas production for commercialLiFePO4 batteries during overcharge-thermal runaway, J. Energy Storage 72 (2023) 108323, http://dx.doi.org/10.1016/j.est.2023.108323, URL https://www.sciencedirect.com/science/article/pii/S2352152X23017206.

[67] E.P. Roth, C.J. Orendorff, How electrolytes influence battery safety, Electrochem. Soc. Interface 21 (2) (2012) 45, http://dx.doi.org/10.1149/2.F04122if.

[68] J. Lamb, C.J. Orendorff, E.P. Roth, J. Langendorf, Studies on the thermal breakdown of common Li-ion battery electrolyte components, J. Electrochem. Soc. 162 (10) (2015) A2131, http://dx.doi.org/10.1149/2.0651510jes.

[69] Y. Fernandes, A. Bry, S. de Persis, Thermal degradation analyses of carbonate solvents used in Li-ion batteries, J. Power Sources 414 (2019) 250–261, http://dx.doi.org/10.1016/j.jpowsour.2018.12.077, URL https://www.sciencedirect.com/science/article/pii/S0378775318314289.

[70] P.J. Bugryniec, S. Vernuccio, S.F. Brown, Towards a micro-kinetic model of Li-ion battery thermal runaway — reaction network analysis of dimethyl carbonate thermal decomposition, J. Power Sources 580 (2023) 233394, http://dx.doi.org/10.1016/j.jpowsour.2023.233394, URL https://www.sciencedirect.com/science/article/pii/S037877532300770X.

[71] Q. Wang, P. Ping, X. Zhao, G. Chu, J. Sun, C. Chen, Thermal runaway caused fire and explosion of lithium ion battery, J. Power Sources 208 (2012) 210–224, http://dx.doi.org/10.1016/j.jpowsour.2012.02.038, URL https://www.sciencedirect.com/science/article/pii/S0378775312003989.

[72] X. Feng, M. Ouyang, X. Liu, L. Lu, Y. Xia, X. He, Thermal runaway mechanism of lithium ion battery for electric vehicles: A review, Energy Storage Mater. 10 (2018) 246–267, http://dx.doi.org/10.1016/j.ensm.2017.05.013, URL https://www.sciencedirect.com/science/article/pii/S2405829716303464.

[73] D.H. Doughty, E.P. Roth, C.C. Crafts, G. Nagasubramanian, G. Henriksen, K. Amine, Effects of additives on thermal stability of Li ion cells, J. Power Sources 146 (1) (2005) 116–120, http://dx.doi.org/10.1016/j.jpowsour.2005.03.170, URL https://www.sciencedirect.com/science/article/pii/S0378775305005057 Selected papers pressented at the 12th International Meeting on Lithium Batteries.

[74] F. Zheng, M. Kotobuki, S. Song, M.O. Lai, L. Lu, Review on solid electrolytes for all-solid-state lithium-ion batteries, J. Power Sources 389 (2018) 198–213, http://dx.doi.org/10.1016/j.jpowsour.2018.04.022, URL https://www.sciencedirect.com/science/article/pii/S0378775318303653.

[75] D. Sturk, L. Hoffmann, A.A. Tidblad, Fire tests on E-vehicle battery cells and packs, Traffic Inj. Prev. 16 (sup1) (2015) S159–S164, http://dx.doi.org/10.1080/15389588.2015.1015117.

[76] F. Larsson, P. Andersson, P. Blomqvist, B.-E. Mellander, Toxic fluoride gas emissions from lithium-ion battery fires, Sci. Rep. 7 (1) (2017) 10018, http://dx.doi.org/10.1038/s41598-017-09784-z.

[77] Z. Huang, C. Zhao, H. Li, W. Peng, Z. Zhang, Q. Wang, Experimental study on thermal runaway and its propagation in the large format lithium ion battery module with two electrical connection modes, Energy 205 (2020) 117906, http://dx.doi.org/10.1016/j.energy.2020.117906, URL https://www.sciencedirect.com/science/article/pii/S0360544220310136.

[78] T. Zhou, J. Sun, J. Li, S. Wei, J. Chen, S. Dang, N. Tang, Y. Zhu, Y. Lian, J. Guo, F. Zhang, H. Xie, H. Li, X. Qiu, L. Chen, Toxicity, emissions and structural damage from lithium-ion battery thermal runaway, Batteries 9 (6) (2023) http://dx.doi.org/10.3390/batteries9060308, URL https://www.mdpi.com/2313-0105/9/6/308.

[79] F. Larsson, P. Andersson, B.-E. Mellander, Lithium-ion battery aspects on fires in electrified vehicles on the basis of experimental abuse tests, Batteries 2 (2) (2016) http://dx.doi.org/10.3390/batteries2020009, URL https://www.mdpi.com/2313-0105/2/2/9.

[80] C.F. Larsson, P. Andersson, P. Blomqvist, B.-E. Mellander, Gas emissions from lithium-ion battery cells undergoing abuse from external fire, in: Fires in Vehicles (FIVE) 2016 Conference Proceedings, Vol. 2016, 2016, 2016, pp. 253–256, URL https://research.chalmers.se/en/publication/243272.

[81] J. Sun, J. Li, T. Zhou, K. Yang, S. Wei, N. Tang, N. Dang, H. Li, X. Qiu, L. Chen, Toxicity, a serious concern of thermal runaway from commercial Li-ion battery, Nano Energy 27 (2016) 313–319, http://dx.doi.org/10.1016/j.nanoen.2016.06.031, URL https://www.sciencedirect.com/science/article/pii/S2211285516302130.

[82] P. Andersson, P. Blomqvist, A. Lorèn, F. Larsson, Investigation of Fire Emissions from Li-Ion Batteries, SP Technical Research Institute of Sweden, 2013, URL https://www.diva-portal.org/smash/get/diva2:962743/FULLTEXT01.pdf.

[83] G. Siegemund, W. Schwertfeger, A. Feiring, B. Smart, F. Behr, H. Vogel, B. McKusick, Fluorine compounds, organic, in: Ullmann's Encyclopedia of Industrial Chemistry, John Wiley & Sons, Ltd, 2000, p. 461, http://dx.doi.org/10.1002/14356007.a11_349, arXiv:https://onlinelibrary.wiley.com/doi/pdf/10.1002/14356007.a11_349 URL https://onlinelibrary.wiley.com/doi/abs/10.1002/14356007.a11_349.

[84] S. Ogunfuye, H. Sezer, A.O. Said, A. Simeoni, V. Akkerman, An analysis of gas-induced explosions in vented enclosures in lithium-ion batteries, J. Energy Storage 51 (2022) 104438, http://dx.doi.org/10.1016/j.est.2022.104438, URL https://www.sciencedirect.com/science/article/pii/S2352152X22004613.

[85] N.P. Lebedeva, L. Boon-Brett, Considerations on the chemical toxicity of contemporary Li-ion battery electrolytes and their components, J. Electrochem. Soc. 163 (6) (2016) A821, http://dx.doi.org/10.1149/2.0171606jes.

[86] Federal Emergency Management Agency, U.S. Department of Transportation, U.S Environmental Protection Agency, Handbook Of Chemical Hazard Analysis Procedures, National Service Center for Environmental Publications (NSCEP), 1989, URL https://nepis.epa.gov/Exe/ZyPURL.cgi?Dockey=10003MK5.txt.

[87] A.A. Abd-El-Latif, P. Sichler, M. Kasper, T. Waldmann, M. Wohlfahrt-Mehrens, Insights into thermal runaway of Li–Ion cells by accelerating rate calorimetry coupled with external sensors and online gas analysis, Batter. Supercaps 4 (7) (2021) 1135–1144, http://dx.doi.org/10.1002/batt.202100023, arXiv:https://chemistry-europe.onlinelibrary.wiley.com/doi/pdf/10.1002/batt.202100023 URL https://chemistry-europe.onlinelibrary.wiley.com/doi/abs/10.1002/batt.202100023.

[88] M. Lammer, A. Königseder, V. Hacker, Holistic methodology for characterisation of the thermally induced failure of commercially available 18650 lithium ion cells, RSC Adv. 7 (2017) 24425–24429, http://dx.doi.org/10.1039/C7RA02635H.

[89] M. Lammer, A. Königseder, P. Gluschitz, V. Hacker, Influence of aging on the heat and gas emissions from commercial lithium ion cells in case of thermal failure, J. Electrochem. Sci. Eng. 8 (1) (2018) 101–110, http://dx.doi.org/10.5599/jese.476, URL https://pub.iapchem.org/ojs/index.php/JESE/article/view/476.

[90] M. Karp, Heat rate and vent gas analysis thermal runaway vent gas analysis of 18650 and pouch cell, in: 9th Triennial Fire and Safety Cabin Conference, 2019, URL https://www.fire.tc.faa.gov/2019Conference/files/Battery_V/KarpThermalRunawayAnalysis/KarpHeatRateandVentGasAnalysis.pdf.

[91] C. Essl, A.W. Golubkov, A. Fuchs, Influence of aging on the failing behavior of automotive lithium-ion batteries, Batteries 7 (2) (2021) http://dx.doi.org/10.3390/batteries7020023, URL https://www.mdpi.com/2313-0105/7/2/23.

[92] T. Ohsaki, T. Kishi, T. Kuboki, N. Takami, N. Shimura, Y. Sato, M. Sekino, A. Satoh, Overcharge reaction of lithium-ion batteries, J. Power Sources 146 (1) (2005) 97–100, http://dx.doi.org/10.1016/j.jpowsour.2005.03.105, URL https://www.sciencedirect.com/science/article/pii/S0378775305005112 Selected papers pressented at the 12th International Meeting on Lithium Batteries.

[93] Q. Yuan, F. Zhao, W. Wang, Y. Zhao, Z. Liang, D. Yan, Overcharge failure investigation of lithium-ion batteries, Electrochim. Acta 178 (2015) 682–688, http://dx.doi.org/10.1016/j.electacta.2015.07.147, URL https://www.sciencedirect.com/science/article/pii/S0013468615302140.

[94] K.C. Abbott, J.E. Buston, J. Gill, S.L. Goddard, D. Howard, G.E. Howard, E. Read, R.C. Williams, Experimental study of three commercially available 18650 lithium ion batteries using multiple abuse methods, J. Energy Storage 65 (2023) 107293, http://dx.doi.org/10.1016/j.est.2023.107293, URL https://www.sciencedirect.com/science/article/pii/S2352152X23006904.

[95] C.M. Vendra, A.V. Shelke, J.E. Buston, J. Gill, D. Howard, E. Read, A. Abaza, B. Cooper, J.X. Wen, Numerical and experimental characterisation of high energy density 21700 lithium-ion battery fires, Process Saf. Environ. Prot. 160 (2022) 153–165, http://dx.doi.org/10.1016/j.psep.2022.02.014, URL https://www.sciencedirect.com/science/article/pii/S0957582022001082.

[96] E.V. FireSafe, Mercedes Vito electric van in thermal runaway near Heathrow Airport, 2023, video URL https://www.youtube.com/watch?v=mIIdMkwKLp4.

[97] R.W. Kennedy, K.C. Marr, O.A. Ezekoye, Gas release rates and properties from lithium cobalt oxide lithium ion battery arrays, J. Power Sources 487 (2021) 229388, http://dx.doi.org/10.1016/j.jpowsour.2020.229388, URL https://www.sciencedirect.com/science/article/pii/S0378775320316724.

[98] C.C. Crafts, D.H. Doughty, J. McBreen, E.P. Roth, Advanced technology development program for lithium-ion batteries : thermal abuse performance of 18650 Li-ion cells, 2004, http://dx.doi.org/10.2172/918751, URL https://www.osti.gov/biblio/918751.

[99] M. Karp, Lithium ion thermal runaway less than 2 wh lithium ion batteries, in: International Aircraft Systems Fire Protection Working Group, FAA, 2017, URL https://www.fire.tc.faa.gov/pdf/systems/Nov17Meeting/Karp-1117-2WhBatteries.pdf.

[100] FAA Fire Safety, Solid state battery tests, 2017, URL https://www.fire.tc.faa.gov/pdf/systems/Nov17Meeting/Maloney-1117-Solid_State_battery_tests.pdf.

[101] S. Chen, Z. Wang, J. Wang, X. Tong, W. Yan, Lower explosion limit of the vented gases from Li-ion batteries thermal runaway in high temperature condition, J. Loss Prev. Process Ind. 63 (2020) 103992, http://dx.doi.org/10.1016/j.jlp.2019.103992, URL https://www.sciencedirect.com/science/article/pii/S0950423018309744.

[102] Z. Huang, X. Li, Q. Wang, Q. Duan, Y. Li, L. Li, Q. Wang, Experimental investigation on thermal runaway propagation of large format lithium ion battery modules with two cathodes, Int. J. Heat Mass Transfer 172 (2021) 121077, http://dx.doi.org/10.1016/j.ijheatmasstransfer.2021.121077, URL https://www.sciencedirect.com/science/article/pii/S0017931021001800.

[103] J. Hynynen, O. Willstrand, P. Blomqvist, P. Andersson, Analysis of combustion gases from large-scale electric vehicle fire tests, Fire Saf. J. 139 (2023) 103829, http://dx.doi.org/10.1016/j.firesaf.2023.103829, URL https://www.sciencedirect.com/science/article/pii/S0379711223000978.

[104] W.Q. Walker, Characterization of the GS YUASA 134 ah cell thermal runaway events with large format fractional thermal runaway calorimetry (L-FTRC), 2020, URL https://www.nasa.gov/sites/default/files/atoms/files/nabw20_char_gsy134_tr_l-ftrc_wwalker.pdf.

[105] P. Bugryniec, S. Vernuccio, S. Brown, Predicting the evolution of flammable gases during li-ion battery thermal runaway using micro-kinetic modelling, in: A.C. Kokossis, M.C. Georgiadis, E. Pistikopoulos (Eds.), 33rd European Symposium on Computer Aided Process Engineering, in: Computer Aided Chemical Engineering, vol. 52, Elsevier, 2023, pp. 1077–1082, http://dx.doi.org/10.1016/B978-0-443-15274-0.50172-4, URL https://www.sciencedirect.com/science/article/pii/B9780443152740501724.

[106] J.M. Kuchta, Investigation of Fire and Explosion Accidents in the Chemical, Mining, and Fuel-Related Industries - A Manual, Techreport Bulletin 68, U.S. Bureau of Mines, 1985.

[107] Battery University, Lithium-ion safety concerns, 2022, URL https://batteryuniversity.com/article/lithium-ion-safety-concerns. (Accessed 30 January 2024).

[108] Renogy, Are lithium ion batteries dangerous and what are the safest lithium batteries?, 2022, URL https://www.renogy.com/blog/are-lithium-ion-batteries-dangerous-and-what-are-the-safest-lithium-batteries/. (Accessed 30 January 2024).

[109] LithiumWerks, Lithium iron phosphate: The safer chemistry, 2024, URL https://lithiumwerks.com/products/technology/safety/. (Accessed 30 January 2024).

[110] relionbattery, How are LiFePO4 batteries safer than other lithium batteries?, 2024, URL https://www.relionbattery.com/knowledge/how-are-lifepo4-batteries-safer-than-other-lithium-batteries. (Accessed 30 January 2024).

[111] V. Ruiz, A. Pfrang, A. Kriston, N. Omar, P. Van den Bossche, L. Boon-Brett, A review of international abuse testing standards and regulations for lithium ion batteries in electric and hybrid electric vehicles, Renew. Sustain. Energy Rev. 81 (2018) 1427–1452, http://dx.doi.org/10.1016/j.rser.2017.05.195, URL https://www.sciencedirect.com/science/article/pii/S1364032117308250.

[112] P.J. Bugryniec, J.N. Davidson, D.J. Cumming, S.F. Brown, Pursuing safer batteries: Thermal abuse of LiFePO4 cells, J. Power Sources 414 (2019) 557–568, http://dx.doi.org/10.1016/j.jpowsour.2019.01.013.

[113] D.H. Doughty, C.C. Crafts, FreedomCAR: Electrical Energy Storage System Abuse Test Manual for Electric and Hybrid Electric Vehicle Applications, Tech. Rep., sAND2005-3123, Sandia National Laboratories, 2006, http://dx.doi.org/10.2172/889934.

[114] Z. Wang, J. Yuan, X. Zhu, H. Wang, L. Huang, Y. Wang, S. Xu, Overcharge-to-thermal-runaway behavior and safety assessment of commercial lithium-ion cells with different cathode materials: A comparison study, J. Energy Chem. 55 (2021) 484–498, http://dx.doi.org/10.1016/j.jechem.2020.07.028, URL https://www.sciencedirect.com/science/article/pii/S2095495620305234.

[115] International Energy Agency, Global EV Outlook 2023, Tech. Rep., International Energy Agency, 2023, p. 57, URL https://www.iea.org/reports/global-ev-outlook-2023.